European Heart Journal Advance Access published May 4, 2016

European Heart Journal
doi:10.1093/eurheartj/ehw140

REVIEW

Clinical update

Taxonomy of segmental myocardial systolic dysfunction

Adam K. McDiarmid[1], Pierpaolo Pellicori[2], John G. Cleland[2], and Sven Plein[1]*

[1]Multidisciplinary Cardiovascular Research Centre & Division of Biomedical Imaging, Leeds Institute of Cardiovascular and Metabolic Medicine, University of Leeds, Leeds LS2 9JT, UK; and [2]Academic Cardiology Unit, University of Hull, Castle Hill Hospital, Kingston upon Hull, UK

Received 3 November 2015; revised 9 March 2016; accepted 10 March 2016

The terms used to describe different states of myocardial health and disease are poorly defined. Imprecision and inconsistency in nomenclature can lead to difficulty in interpreting and applying trial outcomes to clinical practice. In particular, the terms 'viable' and 'hibernating' are commonly applied interchangeably and incorrectly to myocardium that exhibits chronic contractile dysfunction in patients with ischaemic heart disease. The range of inherent differences amongst imaging modalities used to define myocardial health and disease add further challenges to consistent definitions. The results of several large trials have led to renewed discussion about the classification of dysfunctional myocardial segments. This article aims to describe the diverse myocardial pathologies that may affect the myocardium in ischaemic heart disease and cardiomyopathy, and how they may be assessed with non-invasive imaging techniques in order to provide a taxonomy of myocardial dysfunction.

Keywords Taxonomy • Systolic dysfunction • Heart failure • Non-invasive imaging

Introduction

Studies have demonstrated the benefits of pharmacological[1–8] and device interventions[9] for patients with left ventricular systolic dysfunction (LVSD) of ischaemic origin. While there are clear theoretical benefits in improving blood supply to large areas of dysfunctional 'viable' myocardium, several recent clinical trials have failed to demonstrate improved outcomes following revascularization.[10–12]

One explanation for these results may be the terminology employed to describe myocardial health. In particular the terms 'viable' and 'hibernating' are often used interchangeably and sometimes incorrectly. 'Viable' is a summative term used to describe a range of myocardial states including both normal and diseased segments that nonetheless contain a substantial number of cardiac myocytes. Viable myocardial segments can thus include partial thickness scar with fairly normal cardiac myocyte function in the residual portion or myocytes that exhibit contractile dysfunction or failure. On the other hand, 'hibernating' myocardium refers only to the latter subgroup and can be narrowly defined as chronically dysfunctional, ischaemic myocardium that recovers contractile function following improvement in myocardial perfusion limitation. It follows that assessment of 'viability' can be made, to a large degree, prior to revascularization, but identification of 'hibernation' may only be retrospective. Furthermore, identifying myocardium as 'viable' does not necessarily imply 'hibernation' or functional recovery following revascularization, as is sometimes assumed.

A second challenge in the taxonomy of myocardial dysfunction is that it may be assessed with a range of non-invasive imaging techniques. The available techniques differ fundamentally in methodology, the properties of acquired images and the tests' limitations. Therefore, discrepancies between the modalities are inevitable, making consistency in the definition of myocardial states across imaging fields challenging. Understanding these differences is imperative, especially in the design and interpretation of studies to determine the role of revascularization in patients with long-standing LVSD.

This article creates a clinical taxonomy for the different states of myocardium that may exist and coexist in ischaemic heart disease and cardiomyopathy with reference to histology and non-invasive imaging techniques.

* Corresponding author. Tel: +44 113 3437720, Fax: +44 113 3436603, Email: s.plein@leeds.ac.uk

Available imaging techniques

Non-invasive imaging techniques assess different aspects of myocardial health: function and morphology, perfusion, metabolism, and tissue characterization (*Table 1*).

Function and morphology

Echocardiography provides real-time cine assessment of cardiac structure, myocardial wall thickness, and contractile function. Tissue Doppler imaging (TDI) adds quantification of myocardial motion and global longitudinal strain can be used to detect subtle systolic and diastolic abnormalities that may have greater prognostic value compared with LVEF.[13,14] Cardiac magnetic resonance (CMR) produces high-resolution morphological and cine images of the heart in unrestricted imaging planes and with high accuracy and reproducibility.[15,16] In addition, cine CMR with tissue tagging or feature tracking analysis allows quantitative assessment of segmental contractile function. Both echocardiography and CMR can be combined with pharmacological (dobutamine) or physiological (treadmill/static bike) stress to detect ischaemia and viable, dysfunctional myocardium[17,18] through demonstration of contractile reserve. Single photon emission computed tomography (SPECT) and positron emission tomography (PET) can provide information on global and regional contractile function, but at a lower resolution than echocardiography and CMR. Nuclear techniques are less suited than echocardiography and CMR to measure wall thickness. With all imaging techniques, assessment of segmental contractile reserve is significantly limited by adjacent wall motion abnormalities due to 'tethering'.[19]

Perfusion

Myocardial contrast echocardiography is used to measure perfusion by observing the distribution of intravascular microbubbles in the myocardium and provides a surrogate of myocardial blood flow.[20] Myocardial perfusion CMR tracks the myocardial passage of predominantly extracellular paramagnetic contrast agents[21] and allows estimation of absolute myocardial flow (MBF) and myocardial perfusion reserve (MPR).[22] Single photon emission computed tomography and PET detect perfusion defects through a reduction of signal from radionucleotide bound perfusion tracers in the region of interest[23]; PET is considered the 'gold-standard' for quantitation of MBF and MPR (*Figures 1–3*).

Metabolism

The principal method for metabolic myocardial imaging is currently PET, which allows myocardial metabolic substrate utilization to be characterized and quantified. Magnetic resonance spectroscopy is a less widely used method to interrogate myocardial energetics.

Tissue characterization

Non-invasive tissue characterization is predominantly performed with CMR. Late gadolinium enhancement (LGE) CMR allows identification of scar and focal fibrosis. T1 and extracellular volume (ECV) measurement appears a useful and reproducible surrogate for diffuse myocardial fibrosis,[24,25] while T2-weighted CMR provides assessment of myocardial oedema. Integrated back-scatter echocardiography, which provides assessment of tissue fibrosis might also be applied in this context.

Future directions

Hybrid systems that combine anatomical with perfusion or metabolic imaging (e.g. PET/MR) are becoming available whilst molecular imaging may soon allow identification of specific biological processes.

Taxonomy for myocardial segments

(1) Normal
(2) Ischaemic
  (i) Reversible ischaemia
    (a) Acute prolonged ischaemia
    (b) Chronic intermittent ischaemia
  (ii) Stunning
  (iii) Hibernation
  (iv) Infarction
(3) Myopathic

Normal

Definition: Normal myocardium is by definition viable and metabolically active with normal contractile function and exhibiting contractile reserve in response to increased demand.

Metabolism: Normal cardiac function, including contraction, relaxation, and ionic regulation, is dependent upon adenosine triphosphate (ATP) metabolism. The majority of ATP consumption occurs in myo-fibrils throughout the cardiac cycle. Further ATP is used to regulate sarcolemmal calcium and, at the membrane, Na^+/K^+ ATPase transporter.[26,27] The heart consumes ATP rapidly and is dependent upon constant renewal of ATP, which in turn is dependent upon creatine phosphate levels. Were ATP production to cease and consumption to continue unchecked, cardiac stores would be depleted in ~10–15 s.[26] There are three main pathways by which ATP is synthesised: fatty acid oxidation, ketone body, and carbohydrate metabolism. Fatty acid oxidation yields the most ATP, though all pathways share a common endpoint of mitochondrial ATP synthesis.[28] In situations of increased metabolic demands, the proportion of ATP derived from carbohydrate metabolism increases (*Figure 4*).[27]

Histology: More than 70% of left ventricle (LV) myocardial tissue volume is cardiac myocytes; the rest is vasculature and extra cellular matrix (ECM).[29] Predominantly containing collagen types I and III, ECM composition is regulated by a number of factors, including circulating neuro-hormones and mechanical strain.[30,31]

Imaging, morphology, and function: The LV is a conical structure that tapers from base to apex. The normal LV wall has a thickness of between 6 and 10 mm in men, and 6 and 9 mm in women,[32] in diastole and thickens uniformly by at least 50% in systole. In response to increasing demand, contraction becomes increasingly dynamic.

As well as function, it is also possible to assess the constituents of myocardium and tissue homogeneity. By CMR the signal in healthy myocardium is uniform on T1 and T2 weighted and contrast enhanced images. Semi-quantitative assessment of the ratio of T2 signal in healthy heart to skeletal muscle is <1.9.[33] Quantitative

Table 1 Summary of key imaging modalities, and aspects assessed in defining myocardial

	Morphology and resting function	Stress function/contractile reserve	Perfusion	Metabolism	Tissue characterization
Echo					
Strengths	Readily assessed in a range of situations. Widely accessible Doppler, tissue Doppler, and GLS provide additional important indices Contrast improves accuracy*	Physiological or pharmacological stressors may be employed			Crude visual assessment of scar, Maybe quantified with integrated background scatter (not in routine clinical practice)
Weaknesses	Limited by habitus and lung disease Greater inter-observer variation and less reproducible than CMR**	Affected by tethering in the presence of multiple wall motion abnormalities	Microbubble perfusion remains predominantly a research tool Potential lack of local expertise	Not assessed	
CMR					
Strengths	Multiplanar imaging with excellent reproducibility# Myocardial mechanics may be assessed as per tissue Doppler	Physiological or pharmacological stressors may be employed Highly reproducible	Visual assessment Quantification of perfusion reserve possible Excellent spatial resolution		Focal scar identified with LGE Quantification of fibrosis (T1 mapping) and oedema (T2 mapping)
Weaknesses	Less accessible than echo Unsuitable in critical illness Limited by presence of some implantable cardiac devices & extreme obesity	Stress limitations similar to echo Exercise stressless practical Availability	Absolute quantification of perfusion Standard perfusion not 'whole heart' coverage Gadolinium CI if eGFR $<$ 30 mL/min/1.73 m^2	Not assessed in clinical routine practice, MRS available in some centres	
SPECT					
Strengths	Assessment of systolic function possible during gated perfusion examination		Whole heart coverage Perfusion defect size may be quantified		
Weakness	Other aspects of cardiac function not assessed	Not assessed	Quantitative assessment not possible Lower spatial resolution than PET and CMR Potential imitations in balanced ischaemia‡‡‡ Ionising radiation	Not assessed	Inferred only—scar over estimated‡‡
PET					
Strengths			Gold standard for perfusion quantification Excellent spatial resolution Whole heart coverage	Non-invasive assessment of carbohydrate and lipid metabolism possible	
Weaknesses	Not usually assessed	Not assessed	Exposure to ionising radiation	Exposure to ionising radiation	Tissue composition inferred from metabolism/perfusion findings◇

Symbols: *[136], **[137], #[16,17], ‡‡[139], ‡‡‡[140], ◇[66].

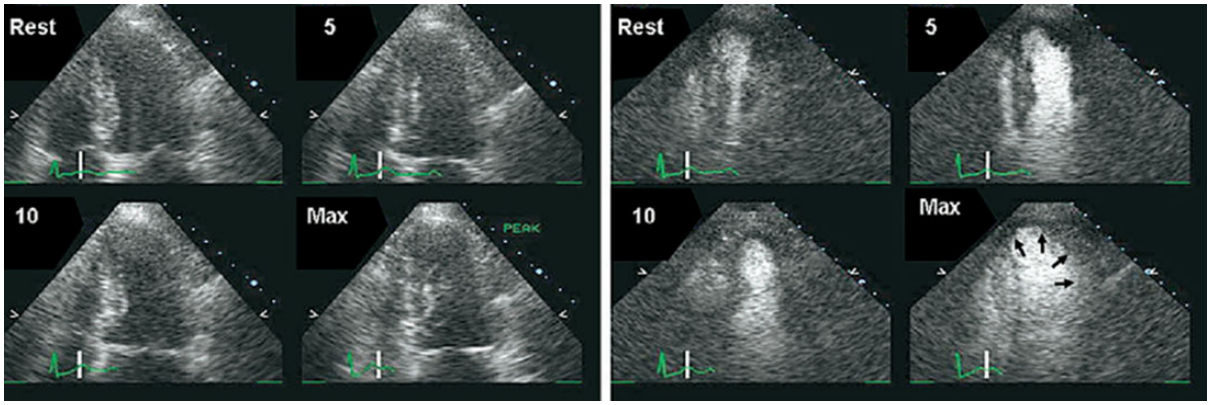

Figure 1 Intra-venous contrast agent use in echocardiography. Left, rest images have poorly defined endocardial border. Right, following administration of intra-venous contrast agent the apical wall motion defect is evident. Taken from Plana *et al.*[141]

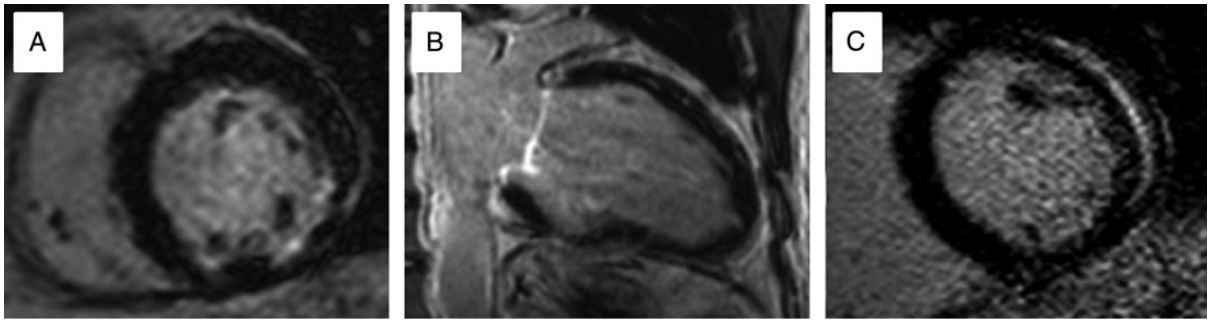

Figure 2 Patterns of late gadolinium enhancement by CMR seen in different pathologies. (*A*) Sub-endocardial infero-lateral enhancement in myocardial infarction. (*B*) Anterior mid wall enhancement in dilated cardiomyopathy. (*C*) Lateral epicardial and pericardial enhancement in myo-pericarditis.

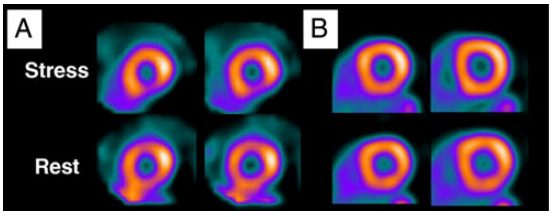

Figure 3 Radionuclide perfusion imaging: (*A*) Hyperaemic stress single photon emission computed tomography and (*B*) positron emission tomography imaging (*B*) of the same patient. (*A*) shows an apparent inferior perfusion defect not present in (*B*) suggesting single photon emission computed tomography attenuation artefact.[50]

measurement of the T1 signal, by T1 mapping, shows normal values in narrowly defined ranges,[34] but depend on scanner field strength and pulse-sequence used.[34]Extracellular volume, calculated using pre- and post-contrast T1 mapping, is less method dependent and is 26 $\pm$ 3% in healthy myocardium.[24]

Nuclear techniques of perfusion and metabolism display uniform signal throughout the myocardium (*Figure 5*). Myocardial perfusion may be quantified both at rest and hyperaemia, allowing calculation of MPR. By PET normal resting MBF is $\sim$0.7 mL/min/g, increasing to 2.75 mL/min/g on stress, with a flow reserve of $>$4.[35] 'Gold-standard' PET flow quantification is not without limitation, especially when the flow reduction is only mild.[36] Estimates of absolute MBF with CMR show limited agreement with PET,[37] though MPR correlates well with PET in health and disease,[37] with normal MPR by CMR being $\sim$2.2.[38]

Ischaemic

Reversible ischaemia

Definition: Myocardial ischaemia is a mismatch of oxygen supply and demand that precipitates change from aerobic to anaerobic cellular respiration.

Metabolism: Ischaemia may either be complete, due to coronary occlusion, or limited due to epicardial coronary artery stenosis or abnormalities of the myocardial microvascular circulation. The degree of ischaemia is also determined by the presence and extent

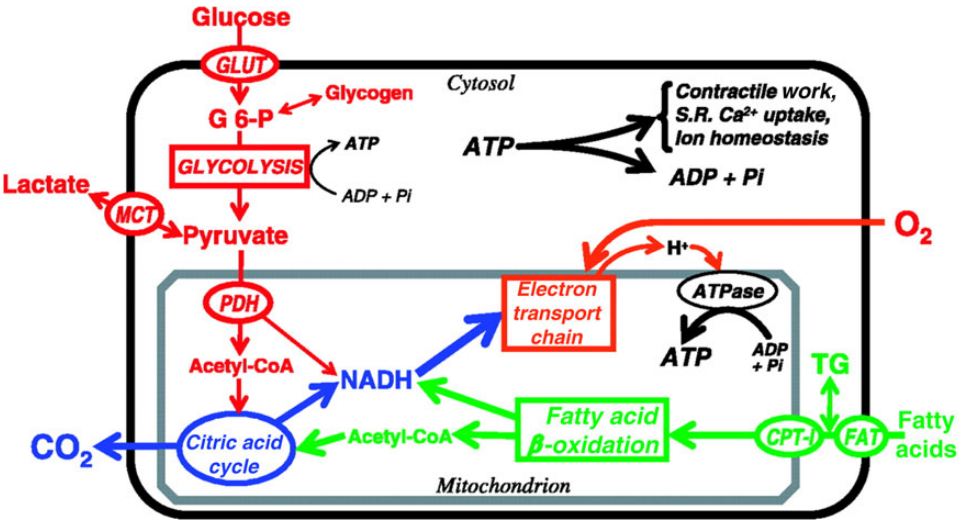

Figure 4 Normal myocyte metabolism: taken from Myocardial Substrate Metabolism in the Normal and Failing Heart.[28]

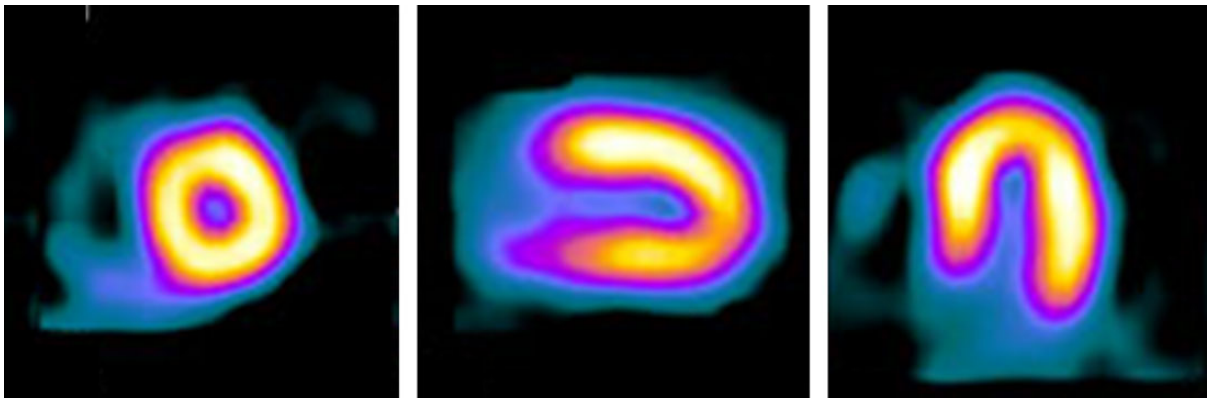

Figure 5 Normal single photon emission computed tomography examination: Left ventricle seen in short axis, vertical long axis, and horizontal long axis. Adapted from Hasegawa *et al.*[142]

of a collateral circulation that can develop in humans with established coronary artery disease.

Changes in cell metabolism begin within one minute of onset of severe ischaemia. Sub-endocardial tissue becomes ischaemic first followed by sub-epicardial tissue.[39] Shortly after the onset of severe ischaemia, oxygen present in myocardium is consumed and normal oxidative metabolism ceases. At the same time, electron transport across cell membranes decreases and myocyte contraction becomes impaired. During this initial phase, anaerobic respiration replaces aerobic respiration as the dominant source of ATP, and glycogen replaces fatty acids and glucose as the substrate for energy production.[26] Anaerobic respiration in this setting provides approximately one-quarter of the amount of ATP as aerobic metabolism. Due to adverse intra-cellular conditions, including falling pH, ATP production at this rate is only sustained for ~1 min before continuing at a much lower rate for up to 1 h.[26]

In non-severe ischaemia, a degree of aerobic respiration continues, consequently more ATP is produced compared with anaerobic glycolysis. Furthermore, hydrogen ions and lactate that accumulate in severe ischaemia are produced less quickly, and 'washed out' of still perfused tissue, preserving a more physiological environment.

Once ischaemia has resolved, recovery of normal function is variable. Abnormalities of systolic function may persist for several days, myocardium that fails to recover normal systolic function immediately is said to be 'stunned'.[40]

Histology: Abnormal function of cell membrane channels leads to myocyte oedema shortly after onset of ischaemia. In addition following short duration of severe ischaemia, depletion of glycogen stores, and the presence of 'I-bands' in myo-fibrils are seen on electron microscopy.[41]

Imaging, morphology, and function

Acute prolonged ischaemia

Shortly following the onset of ischaemia, regional systolic function becomes impaired and may remain so for days after the ischaemic insult.[40] Echocardiography is most commonly used to identify wall motion abnormalities associated with acute ischaemia. Single photon emission computed tomography and PET are rarely used clinically in the setting of acute ischaemia. On CMR, wall motion and thickness are assessed in a similar fashion to echocardiography. In addition, oedema is readily detectable and quantifiable as areas of high signal on T2-weighted images.[42] T1 and T2 mapping may provide similar, quantitative information. The oedematous zone may be quantified to determine the extent of myocardial salvage following intervention, and delineate the 'area at risk'.

Chronic intermittent ischaemia

Exercise or dobutamine stress echocardiography allows detection of ischaemia as well as determining its location and extent.[43] Ischaemic myocardium shows reduced contractile reserve with regional wall motion abnormalities developing at increasing levels of stress (*Figure 6*).

Cardiac magnetic resonance also allows detection of ischaemia through assessment of regional systolic function. Tissue perfusion can be assessed using first pass adenosine stress CMR (*Figure 7*). Quantitative assessment of perfusion with CMR has limited agreement with PET imaging[44] and is less commonly used in clinical practice than qualitative assessment.

Single photon emission computed tomography is commonly used in the investigation of chronic intermittent ischaemia, and while image quality on PET is superior to SPECT, availability of PET limits utility. The sensitivity and specificity of SPECT compare well with other non-invasive imaging techniques[45]; whole heart acquisition allows accurate quantification of the extent of ischaemia, a measure that may have prognostic value.[46] Image interpretation may be limited by attenuation artefact in the inferior wall and anterior wall, especially in women.[47] In addition to perfusion imaging and LV function, transient LV dilation (transient ischaemic dilation—TID) may be appreciated on stress SPECT imaging, marking adverse prognosis.[48] Transient ischaemic dilation may either represent true dilation as a result of severe coronary disease and stunning, or rather may reflect sub-endocardial defects not appreciated on perfusion imaging.[49]

In head-to-head studies, the theoretical advantages of PET over SPECT have been demonstrated.[36,50] As well as detection of ischaemia it is also possible to measure myocardial blood flow with PET,[51] enabling quantitative assessment of myocardial blood flow reserve, which correlates strongly with coronary artery stenosis severity.[52]

Stunning

Definition: Myocardium is 'stunned' when contractile function is depressed following transient ischaemia, prior to a full recovery, and having sustained no irreversible myocyte damage. The mechanism of sustained systolic dysfunction in stunning is incompletely understood. However, it is believed that oxygen free radical formation and elevated myocardial calcium levels may lead to damage of myocardial proteins or sarcoplasmic reticulum.[53]

Metabolism: Sub-epicardial and sub-endocardial myocardial blood flow normalises quickly following restoration of normal coronary flow, however normal myocardial metabolism takes time to recover. Metabolic changes in transient ischaemia, including fall in myocyte ATP, phosphocreatine and pH, take several hours to reverse.[54] Post-ischaemic myocardial oxidative and glucose metabolism remain depressed by ~20% of normal levels for several hours after an ischaemic insult, and take up to 1 week to recover to near normal levels.[55]

Histology: Histological changes reflect sustained ischaemia. In common with metabolic changes, resolving myocardial oedema, myocardial glycogen, and ATP depletion[40] may be detected several days later.

Imaging, morphology, and function: Systolic function of affected segments is impaired in stunning. The speed of recovery of systolic function is variable and may be related to the duration and severity of the ischaemic insult,[40,56,57] Abnormalities of diastolic function, whether assessed by CMR, conventional or tissue Doppler persist beyond systolic abnormalities.[58,59] It is likely that stunning is an under-appreciated phenomenon as functional abnormalities associated with acute ischaemia will often have recovered.

Dobutamine stress echocardiography in reperfused acute MI has been shown to predict recovery of dysfunctional segments with sensitivity and specificity of 86 and 90%, respectively.[60]

Cardiac magnetic resonance demonstrates changes in keeping with ischaemia including high signal on T2-weighted images indicative of oedema, as well as regional systolic and diastolic wall motion abnormalities.

Positron emission tomography FDG metabolism assessment may demonstrate depressed levels of glucose metabolism, but no significant metabolism perfusion mismatch, as in hibernation, is seen.[58]

Hibernation

Definition: Chronically dysfunctional viable myocardium of ischaemic origin that recovers systolic function following revascularization.

The processes underlying the development of hibernation remain unclear, although several mechanisms have been proposed. It is thought that although resting blood flow is normal, coronary flow reserves are low.[61] This leads to repeated episodes of ischaemia and repetitive myocardial stunning, causing a complex series of physiological and structural changes characteristic of hibernation.[62] The abnormalities seen in hibernating myocardium become more pronounced as the duration of hibernation increases.[63,64] The time course of recovery of LV systolic function following revascularization is dependent upon the severity of myocardial change, with some studies suggesting that irreversible remodelling may occur with extended hibernation despite successful revascularization.[64,65] However, it is not known if delayed recovery may occur beyond study duration.[66]

Metabolism: There remains debate regarding the metabolic changes present in hibernation. However, there is evidence to suggest that glucose uptake and utilization are increased and fatty acid metabolism is decreased in hibernating myocardium.[67,68]

Histology: Hibernating myocardium is macroscopically similar to normal myocardium. However, at a microscopic level, there are diffuse changes within the myocyte and extracellular ultrastructure.

All types of collagen increase in the ECM of hibernating segments, and are more than twice that found in normal myocardium when

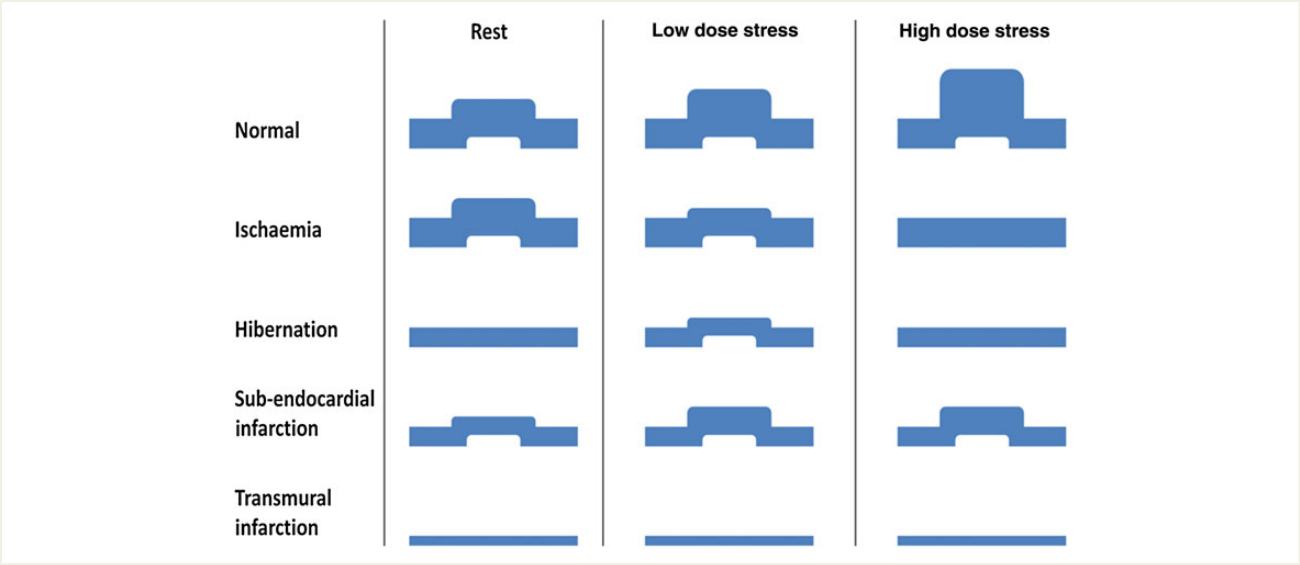

Figure 6 Schematic of wall motion abnormalities in ischaemia, hibernation, sub-endocardial, and infarction.

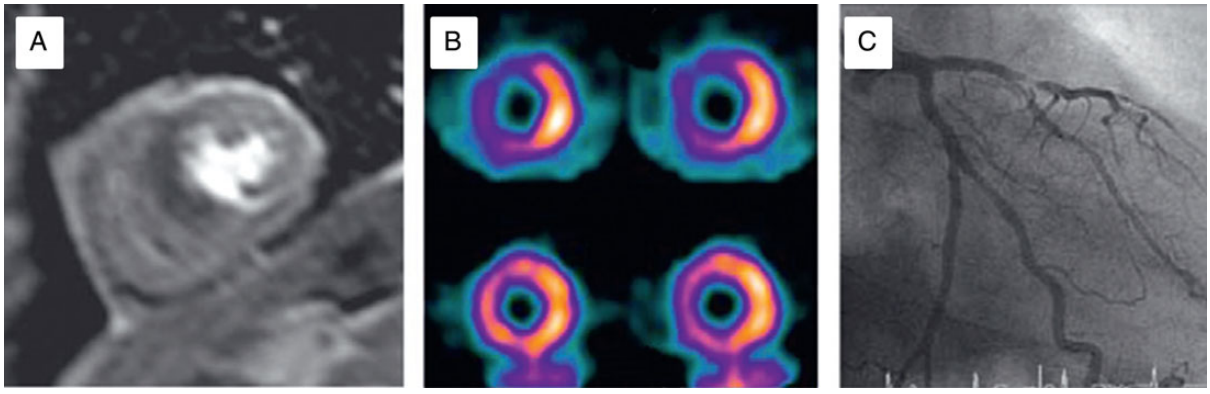

Figure 7 Imaging in chronic ischaemia: (*A*) cardiac magnetic resonance first pass perfusion demonstrating mid-ventricular anterior and septal abnormality. (*B*) Single photon emission computed tomography demonstrating the anterior and septal stress (top row) abnormality that resolves at rest. (*C*) Angiography in the same patient showing severe left anterior descending stenosis. Adapted from Greenwood *et al.* Cardiovascular magnetic resonance and single photon emission computed tomography for diagnosis of coronary heart disease: a prospective trial.[143]

de-differentiation is severe.[62] Structural changes in the ECM become more pronounced as duration of hibernation increases.[64,69] Furthermore, there is down-regulation of myocyte mitochondria and increased glycogen storage when compared with both normal and remote myocardium.[62,68] These changes reflect alteration of mRNA expression and disorganization of cytoskeletal proteins as a result of cellular de-differentiation.

Imaging, morphology, and function: On functional imaging, hibernating myocardium has impaired resting systolic function, and will typically be hypo- or akinetic. Diastolic wall thickness is >6 mm by CMR[70] or 7 mm on trans-thoracic echocardiography,[65] though recent studies have demonstrated that thinning below these thresholds, in the absence of extensive scar, does not preclude recovery.[71] With inotropic stimulation, hibernating myocardium shows 'contractile reserve' or a 'biphasic response', with an improvement in contractile function on low-dose/effort stress prior to deteriorating at higher workloads.[72] Low dose stress TDI allows quantification of systolic function: Doppler tissue velocities increase more in hibernating myocardium than in dysfunctional tissue that does not show improvement in systolic function following revascularization (*Figure 8*).[73,74]

Cardiac magnetic resonance examination allows for accurate assessment of diastolic wall thickness and regional wall motion abnormalities. Late gadolinium enhancement CMR contributes only indirectly to the diagnosis of hibernation. On LGE CMR, hibernating myocardium has the same signal characteristics as normal

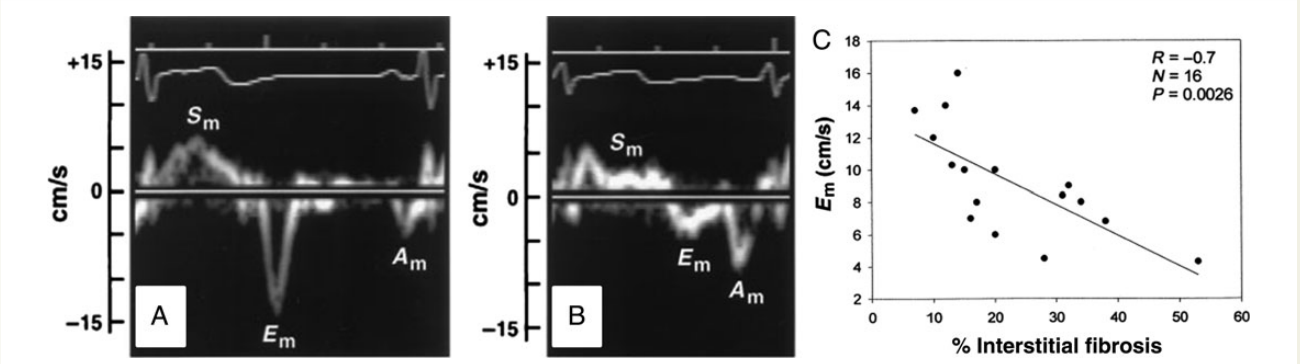

Figure 8 Tissue Doppler in normal *(A)* and chronically ischaemic dysfunctional myocardium *(B)*: E' is related to the degree of interstitial fibrosis adapted from Shan *et al.*[144]

myocardium, with signal uniformly nulled. Late gadolinium enhancement CMR therefore only excludes the presence of myocardial infarction as the cause of contractile dysfunction, suggesting hibernation as one of several potential causes. Absence of LGE in dysfunctional segments in ischaemic heart disease may predict functional recovery following revascularization (*Figure 9*).[75] Cardiac magnetic resonance prediction of recovery can be further enhanced by combined use of functional, LGE, and dobutamine stress imaging. Hibernating myocardium has reduced resting function, the absence of LGE and a biphasic response to dobutamine stress.[72] Finally, myocardial perfusion can be assessed and quantified by first pass CMR. Resting MBF (mL/min/g) is normal in hibernating myocardium, and hyperaemic blood flow is reduced with subsequent improvement following successful revascularization.[76]

In SPECT imaging cellular uptake of Thallium is dependent upon a functional Na^+/K^+ ATPase and preserved sarcolemmal membrane function.[66] In hibernating myocardium, early acquisition following tracer administration identifies a defect, reflecting impaired blood flow on stress, though delayed early uptake may also be evident on rest in severe LV dysfunction.[77] On delayed acquisitions, the isotope has been taken up by metabolically active myocytes in the hibernating region, so the defect is reduced. Stress/redistribution SPECT thus allows quantification of ischaemia and the extent of potential recovery.[78] Technetium-based tracers, which bind within myocytes to mitochondria, identify viable myocardium similarly to Thallium SPECT.

Positron emission tomography assessment is most commonly based on the assessment of myocardial glucose uptake with FDG. Tracer signal is proportional to metabolically active myocardium and likelihood of recovery may be predicted by the glucose metabolic rate (*Figure 10*).[79,80,81] In addition, PET allows the detection and quantification of MPR, which is reduced in hibernation.[82,83]

Hibernation with non-trans-mural scar

Hibernation commonly co-exists in the presence of sub-endocardial infarction and as a consequence overlap of imaging findings may be seen, e.g. sub-endocardial enhancement on LGE CMR, or both fixed and inducible perfusion defects on nuclear study.

In the setting of partial infarction response to dobutamine stress on functional imaging is reduced. Decreased circumferential strain measured by echocardiography further facilitates differentiation of normal myocardium, sub-endocardial, and transmural infarction.[84,85]

The spatial resolution of CMR LGE enables the detection of small volumes of infarction that may be missed by SPECT or PET. Transmural extent of LGE predicts likelihood of systolic recovery: 60% with 1–25% LGE, 42% with 26–50% LGE, and only 7% of segments with >50% enhancement recovered at 3 months in a cohort with predominantly chronic, mild LVSD (LVEF 43%).[75] In a second mixed cohort of acute and chronic patients with moderate LVSD (LVEF 38%) recovery rates were similar (0 LGE:73%, 1–25:56%, 26–50:45%, >50%:5%).[86]

Where hibernation co-exists with acute abnormalities a 'mixed picture' of imaging findings may result. Definitive classification of abnormalities in this setting is difficult and may require repeated imaging to classify myocardium.

Infarction

Definition: Myocardial infarction follows sustained ischaemia leading to myocyte necrosis and subsequent remodelling and fibrosis.

Metabolism: Necrosis occurs when sustained severe ischaemia leads to irreversible structural changes within the myocyte, including mitochondrial swelling and disruption of the sacrolemma.[41] In the course of ischaemic injury, necrosis begins in the sub-endocardium where tissue perfusion is lowest and energy consumption is highest, leading to ATP supply exhaustion and accumulation of the by-products of glycolysis. Sub-endocardial infarction commences ~20 min after ischaemia onset. Prolonged ischaemia leads to increasingly transmural necrosis, which moves as a 'wave front' from the endocardium to the epicardium,[39] though sometimes with sparing of a thin rim of sub-endocardium.

Histology: Characteristic histological changes occur during myocardial infarction, and evolve until the infarcted region undergoes scar replacement. On macroscopic examination there are few detectable changes over the first 4 h. From 4 to 12 h myocardium becomes mottled. Over the next week, the infarct centre becomes pale and yellows while developing red margins, followed by replacement of necrotic infarct by fibrous scar tissue.[87,88]

Figure 9 Increasing transmurality of late gadolinium enhancement predicts lack of response to revascularization in chronically ischaemic dysfunctional myocardium: Progressive transmurality of scar predicts lack of improvement in systolic function following revascularization. (*A*) 25% late gadolinium enhancement of the inferior wall and infer-septum (*B*) 50% late gadolinium enhancement in the infero-lateral wall becoming increasingly transmural inferiorly. (*C*) 100% late gadolinium enhancement of the inferior wall.

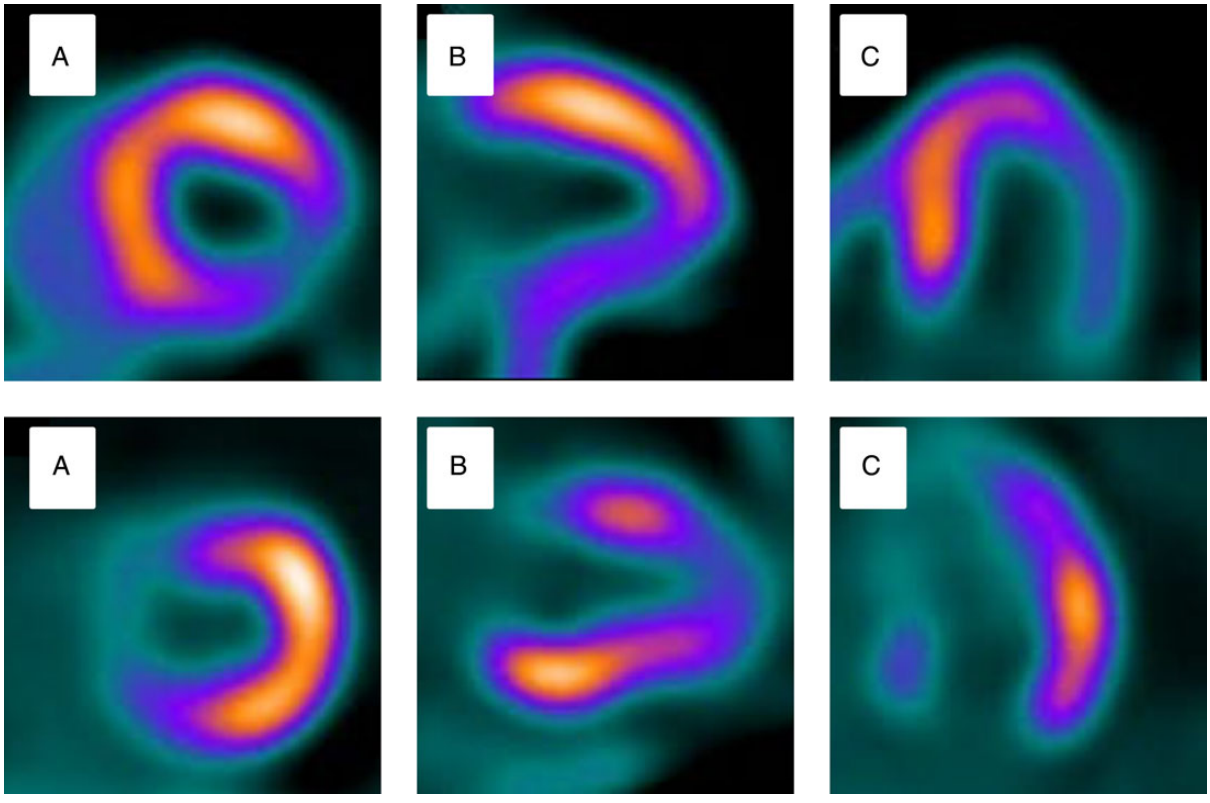

Figure 10 Perfusion-metabolism mismatching on PET in hibernating myocardium: (*A*) Short axis. (*B*) Vertical long axis. (*C*) Horizontal long axis. Top row demonstrates a stress perfusion defect in the infero-lateral wall. Matched metabolism imaging shows preservation of metabolism in the same territory indicating potential hibernation. Adapted from Bengel, Cardiac Positron Emission Tomography.[50]

Microscopically, myocardium undergoes a series of changes responsible for the macroscopically appreciable abnormalities. During the initial phase, glycogen depletion and oedema, in keeping with severe ischaemia is seen on electron microscopy.[89] Between 4 and 12 h, oedema, necrosis, and intra-myocardial haemorrhage are seen. From 12 to 24 h neutrophil infiltration and ongoing necrosis develop. This is followed within 24–48 h by the disappearance of nuclei and striations, and macrophages remove dead cells at the

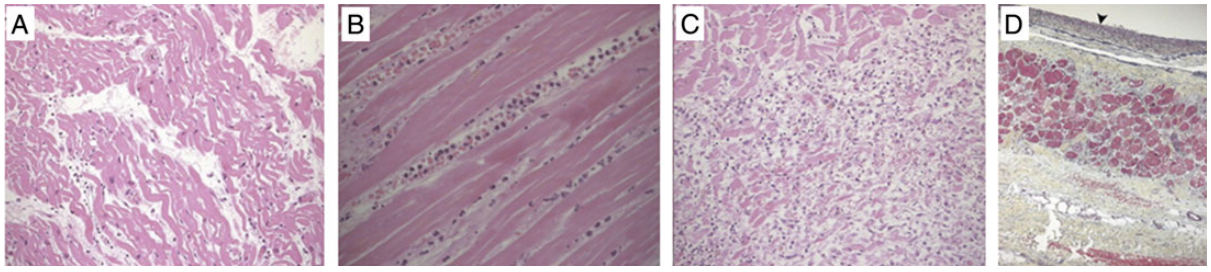

Figure 11 Histological change following myocardial infarction: pathology of myocardial infarction, diagnostic histopathology 2013. (*A*) Light microscopy of wavy mitochondrial fibres and interstitial oedema 4 h postmyocardial infarction. (*B*) Myocardial fibres 24 h post-myocardial infarction, myocardial thinning, and interstitial infiltration by polymorphonuclear leukocytes. (*C*) Granulation tissue 7–10 days post infarction. Near complete removal of myocytes. (*D*) Light microscopy 2–3 weeks after infarction. Subendocardial fibrosis marked by arrowhead, with a small area of myocardial fibre preservation between layers of collagen deposition. Adapted from Chang *et al.*[145]

infarct border. Following this granulation tissue and collagen deposition begins, eventually leading to the formation of collagen scar (*Figure 11*).[90,91]

Imaging, morphology, and function: Wall motion abnormalities develop before ECG changes or symptoms,[92] while TDI systolic velocities decrease rapidly following onset of ischaemia.[93] Following transmural infarction, myocardium is akinetic and thins with time. On stress or exercise there is no improvement in wall thickening with the absence of contractile reserve.[94] Sub-endocardial infarction results in wall motion abnormalities of varying severities, and may be differentiated from transmural infarction using peak systolic circumferential strain and strain rate on stress echocardiography.[95]

Cardiac magnetic resonance demonstrates gross anatomical changes associated with infarction including remodelling, wall thinning, and motion abnormalities.[42] In addition, CMR imaging can be used to delineate infarct extent, indicate the area at risk, and detect microvascular and reperfusion injury.[96,97] Late gadolinium enhancement CMR after acute MI displays high signal in the infarcted area due to persistence of gadolinium within areas of increased extracellular volume and abnormal washout kinetics.[42] In animal models, infarct enhancement with LGE CMR has been observed within 90 min of the onset of ischaemia.[98] In the acute phase, infarct extent may be overestimated due to increased signal and contrast in the oedematous peri-infarct zone.[99] In acute myocardial infarction, LGE CMR may show an area of low signal within the otherwise high-signal infarct zone. This reflects microvascular obstruction (MO) leading to an absence of gadolinium delivery to the centre of the infarct. Extensive MO is associated with no-flow on invasive coronary angiography and adverse LV remodelling.[100] Within an area of MO, myocardial haemorrhage may occur, causing low signal on T2 and T2* CMR.[101] Haemorrhage represents more severe structural change in the setting of acute MI and is also associated with adverse LV remodelling following infarction.[102] The combination of the information gained from T2 weighted, early gadolinium, and late gadolinium images allows measurement of the area at risk, infarct size, and myocardial salvage (difference between area at risk and infarct size) (*Figure 12*).[97]

At the time of acute infarction SPECT imaging is not usually performed. However in research settings, infarct area as delineated by absent tracer uptake on SPECT correlates well with infarct size on pathological specimens.[103] In chronic infarction, metabolically active myocytes are replaced by scar and the absence of an intact Na^+/K^+ ATPase leads to lack of uptake of the SPECT tracer within the region of infarction. The limited spatial resolution of SPECT can lead to an under-appreciation of the extent of infarction because small sub-endocardial infarction may not be detected.[104]

In acute myocardial infarction, FDG PET allows detection of infarction and the presence of viable tissue in or adjacent to the infarcted territory. The absence of detectable glucose metabolism is associated with irreversible myocardial injury.[105] Myocardial perfusion by PET in the acute MI zone is depressed, significantly improves following coronary intervention, and may continue to improve up to 2 weeks later.[106]

In the setting of chronic myocardial infarction, concordant reduction in signal from both perfusion and metabolism (NH3 and FDG tracers, respectively) PET is seen and readily appreciated in transmural infarction; however, in sub-endocardial infarction PET may fail to detect small areas of sub-endocardial scar when compared with CMR.[107]

Myopathic myocardium

Definition: Dysfunctional myocardium of non-ischaemic origin is considered to be myopathic. Myopathy covers a wide range of pathologies. This review will focus on dilated cardiomyopathy, in which pronounced isolated segmental systolic dysfunction is uncommon, with only passing reference to other aetiologies.

Metabolism: Normal cardiac function relies upon matching of energy demand and consumption. This requires an appropriate oxygen supply to myocytes, mitochondrial function, ATP transport to the site of energy consumption, and a reliable feedback system to maintain appropriate metabolic rates. Energy depletion, perhaps due to mitochondrial dysfunction, could be a primary reason for impaired myocardial contraction. However, the primary defect may usually be in the contractile apparatus or in calcium handling, which increase metabolic demand. Importantly, myopathy may be an acquired phenomenon in un-infarcted myocardium that has undergone remodelling and may co-exist alongside segments affected by scar, ischaemia, stunning or hibernation. In patients with mild heart failure secondary

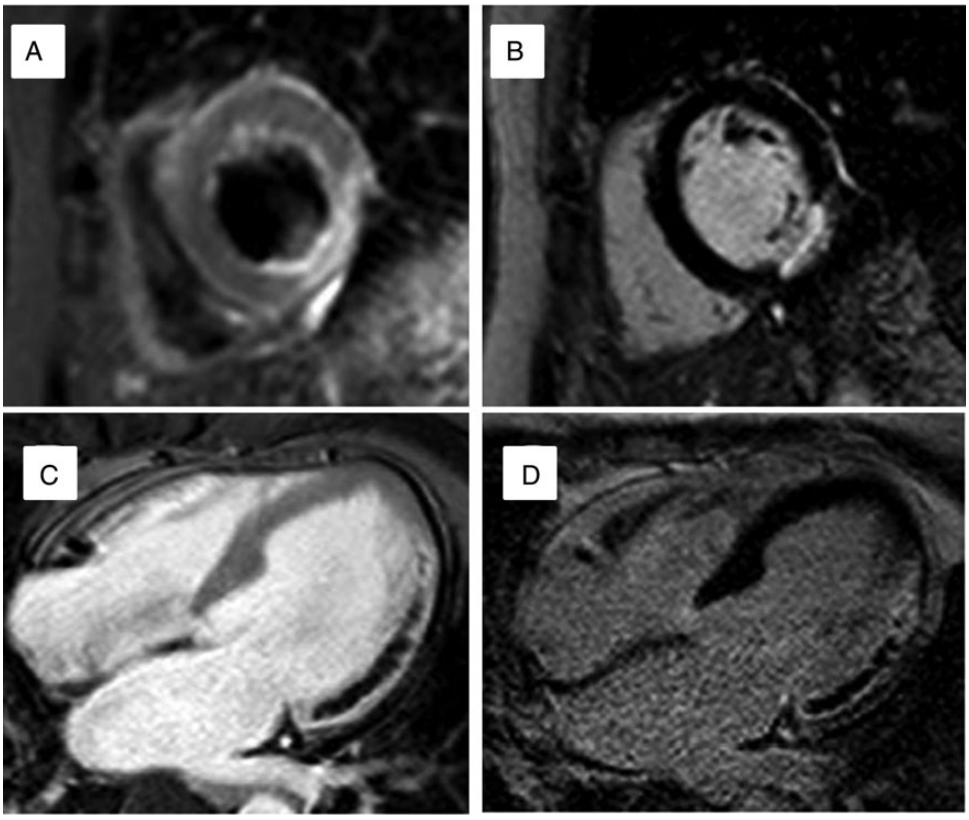

Figure 12 Acute myocardial infarction on cardiac magnetic resonance: Top row: (*A*) High signal on T2-weighted image demonstrating Infero-lateral oedema and 'area at risk'. (*B*) Subendocardial infarction in the same patient on late gadolinium enhancement. Bottom row: (*C*) early gadolinium enhancement image in a second patient with extensive lateral wall hypoenhancement. (*D*) Late gadolinium enhancement confirms infarction and microvascular obstruction.

to idiopathic dilated cardiomyopathy any change myocardial substrate utilization is subtle. In severe heart failure, cellular metabolism changes substantially, with greater glucose and less free fatty acid utilization,[108,109] in most but not all studies.[110]

Histology: Histological abnormalities differ depending on the underlying aetiology including myocyte disarray and interstitial fibrosis[111] in hypertrophic cardiomyopathy (HCM) and fibro-fatty replacement in arrhythmogenic right ventricular cardiomyopathy. A reduction of mitochondria in the failing heart is common.[28] Differing degrees of myocyte hypertrophy are seen depending upon the aetiology of heart failure. However irrespective of aetiology, a common finding is the expansion of the ECM and fibrosis due to local factors and activation[112] of the renin–aldosterone–angiotensin system.[113] Collagen types I and III are the major structural components in the cardiac ECM, providing both tensile strength and elasticity.[114] In the failing heart, collagen synthesis increases (especially type III collagen), leading to accumulation of intercellular collagen, limiting ventricular compliance, myocyte function, and contributing to both systolic and diastolic dysfunction (*Figure 13*).[115,116]

Imaging, morphology, and function: Functional imaging by echocardiography and CMR supplies important information for prognosis and risk stratification including ejection fraction and left ventricular end diastolic dimensions.[117,118]

Comprehensive structural assessment by echocardiography and CMR may guide management and allow diagnosis of the underlying cardiomyopathic process. For example, it is possible to differentiate between morphologically similar cardiomyopathies on echocardiography: Improvement in long-axis function on stress TDI allows differentiation between ischaemic and non-ischaemic cardiomyopathy.[119] In the case of left ventricular hypertrophy, echocardiographic 2D-strain assessment allows differentiation of HCM and hypertensive LV hypertrophy, while TDI enables differentiation of HCM and athlete's heart.[120,121]

Tissue Doppler imaging of the mitral annulus and mitral inflow velocity provides a non-invasive estimate of left atrial pressure.[122] Cardiac magnetic resonance assessment of left atrial transit time also correlates strongly with LV early diastolic pressure.[123]

In many cardiomyopathies, LGE CMR shows characteristics patterns of enhancement. The presence and extent of LGE predicts outcomes in a range of cardiac diseases, including DCM,[124] HCM,[125] and ischaemic heart disease.[126] Extracellular volume calculation allows measurement of both diffuse fibrotic and infiltrative processes that are unreliably assessed with visual analysis alone.[127,128] T2* mapping allows detection and tracking of iron overload cardiomyopathy.[129]

The ability of SPECT alone to differentiate ischaemic from DCM is uncertain as mild stress perfusion defects are commonly seen with

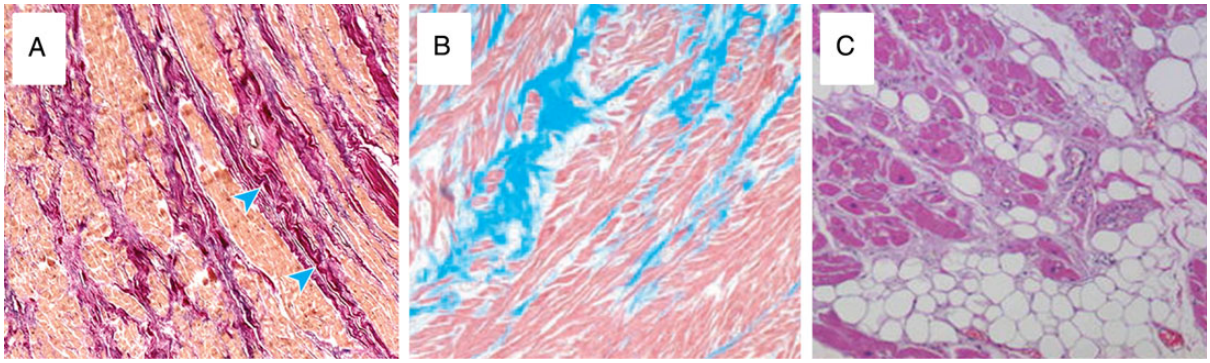

Figure 13 Histological abnormalities in cardiomyopathy: (*A*) Dilated cardiomyopathy, increased interstitial fibrosis at the blue arrow. (*B*) Hypertrophic cardiomyopathy, increased interstitial fibrosis (blue), and myocyte disarray. (*C*) Fibro-fatty replacement in arrhythmogenic right ventricular cardiomyopathy. Taken from Hughes, Asimaki and Saffitz, Gulati.[146–148]

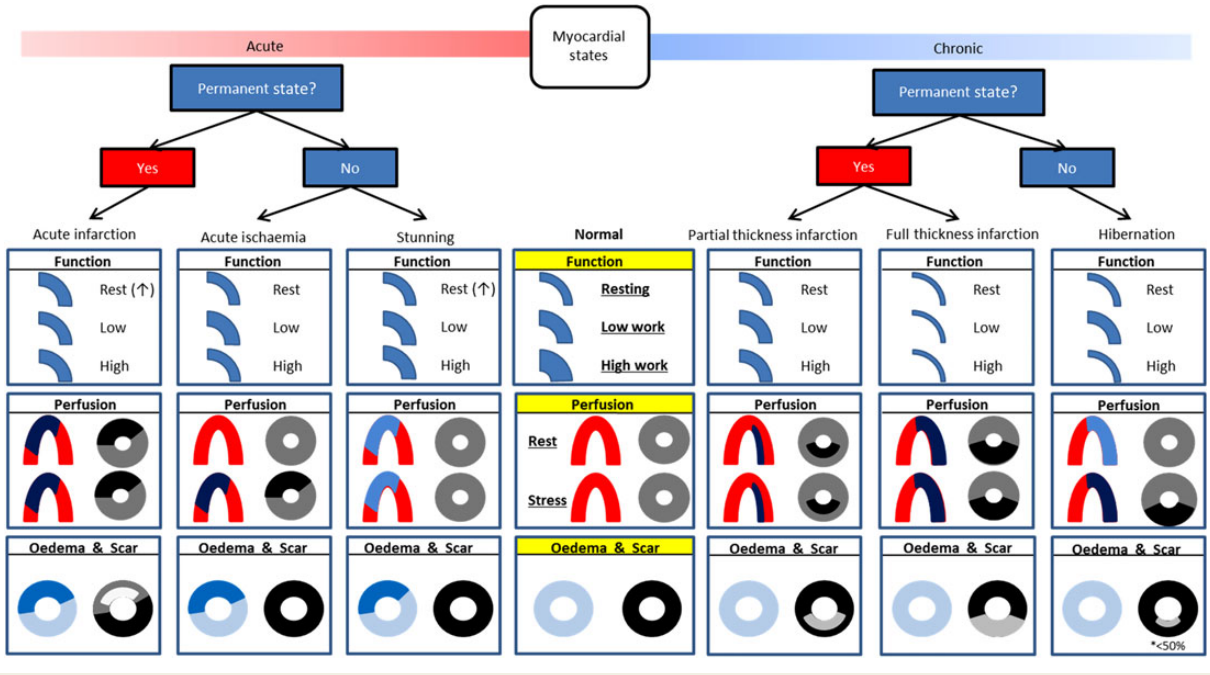

Figure 14 Taxonomy of myocardial segments in left ventricular systolic dysfunction: This should be viewed as an aid to classification rather than a decision tree. Function: thickness compared with 'normal' denotes resting state, with subsequent contractile reserve displayed with increase in segmental thickness. Stunned myocardium may display increased thickness at rest due to oedema though may not be readily appreciable. Perfusion: 'horseshoe' displays typical Single photon emission computed tomography/positron emission tomography finding whilst 'donut' displays cardiac magnetic resonance findings: Single photon emission computed tomography/positron emission tomography: Red = normal; pale blue = minimally decreased or normal; dark blue = decreased. Cardiac magnetic resonance: grey = normal; black=hypoperfusion/ischaemia. Oedema & Scar: 'donut' displays typical T2 weighted (blue) and late gadolinium enhancement findings (black is normal, shades of grey represent late enhancement).

both aetiologies.[130,131] The defects seen have mild stress defect severity ratios (>45%); however, similar abnormalities may be seen in multi-vessel coronary disease precluding the use of SPECT as the sole diagnostic tool in this situation.

Decreased free fatty acid metabolism with increased glucose metabolism is found on PET examination in DCM.[108] Hyperaemic blood flow by PET is lower in DCM than in healthy controls, 2.23 mL/min/mL vs. 4.33 mL/min/mL in one report[132] and perfusion

abnormalities in DCM are progressively worse in more severe heart failure[133] and carry adverse prognosis.[134]

Clinical implications

Different imaging modalities assess different facets of myocardial health and disease and are often complementary. An awareness of the principles underlying acquisition, and the aspect of myocardial health and pathology assessed is crucial.

The detection of 'normal' myocardium is straightforward, and can be accomplished using any test capable of delivering good quality anatomical images. The most appropriate method will vary depending upon patient and institute: In terms of practicality, availability, and economy this will frequently be echocardiography. Atrial as well as ventricular volumes and function should be carefully assessed to detect more subtle disease. Minor deviations from normal, such as small areas of infarction, may be undetected unless high-resolution imaging methods such as LGE CMR are used.

Ischaemia detection or perfusion assessment may be performed using either stress/exercise echo/CMR, CMR first pass perfusion or nuclear imaging, and all are included in current practice guidelines.[135] Single photon emission computed tomography is the most-ly widely used modality worldwide, and PET remains the gold standard. In some patients, it may be desirable to exclude valvular disease or cardiomyopathy making DSE or CMR the most appropriate choice of test.

Hibernation may only ever be identified retrospectively. However, in clinical practice the question most often posed relates to the likelihood of contractile recovery in a given coronary territory, or the potential for LV reverse remodelling following revascularization. For this purpose, any of the non-invasive imaging techniques covered may be selected, as long as the limitations of the chosen technique are recognized in decision making. However, randomized controlled trials have generally not shown a greater improvement in either ventricular function or prognosis with coronary revascularization compared to pharmacological treatment in patients with heart failure and a reduced LV ejection fraction who have greater myocardial viability,[10,11,149] although extended follow of the STICH population recently showed modest 16% reduction in mortality after a median follow-up of 10 years ($p = 0.019$).[150] This may reflect a failure of previous taxonomies rather than a failure of concept; further randomized controlled trials are required.

Partial infarction is best appreciated by CMR examination, with the added benefit that systolic abnormalities not associated with coronary disease may be explained by characteristic abnormalities of cardiomyopathy on LGE CMR.

Where infarction and cardiomyopathy co-exist, multi-modality imaging may be necessary, often including coronary imaging to better understand both the dominant aetiology of LVSD and potential for recovery. Tissue Doppler imaging velocities have been shown to differ in DCM and ischaemic heart disease, potentially allowing discrimination of causes of LVSD. Late gadolinium enhancement CMR allows the extent of scarring due to either pathology to be determined, but not the benefit of any specific therapy.

Mild perfusion defects, with stress defect severity ratios of >45%, are common in DCM as discussed above. SPECT, PET, or CMR first pass perfusion in combination with coronary angiography may facilitate targeted revascularization, if indicated on conventional grounds, and avoiding unnecessary revascularization.

Conclusion

Consistent adoption of standard nomenclature in clinical practice will facilitate thinking and hopefully decision making regardless of local access to different imaging modalities. *Figure 14* summarizes key imaging findings covered and aims to provide a reference for future studies. A clear taxonomy for myocardial viability and dysfunction provides the basis for randomized controlled trials that will provide the scientific evidence upon which to base clinical decisions.

Funding

A.K.M. is funded by a British Heart Foundation (BHF) Project Grant (PG/14/10/30641). S.P. is funded by a BHF Clinical Fellowship (FS/10/62/28409). Funding to pay the Open Access publication charges for this article was provided by The British Heart Foundation (BHF).

Conflict of interest: none declared.

References

1. The Cardiac Insufficiency Bisoprolol Study II (CIBIS-II): a randomised trial. *Lancet* 1999;**353**:9–13.
2. Packer M, Fowler MB, Roecker EB, Coats AJ, Katus HA, Krum H, Mohacsi P, Rouleau JL, Tendera M, Staiger C, Holcslaw TL, Amann-Zalan I, DeMets DL. Effect of carvedilol on the morbidity of patients with severe chronic heart failure: results of the carvedilol prospective randomized cumulative survival (COPERNICUS) study. *Circulation* 2002;**106**:2194–2199.
3. Effect of metoprolol CR/XL in chronic heart failure: Metoprolol CR/XL Randomised Intervention Trial in Congestive Heart Failure (MERIT-HF). *Lancet* 1999;**353**:2001–2007.
4. The SOLVD Investigattors. Effect of enalapril on mortality and the development of heart failure in asymptomatic patients with reduced left ventricular ejection fractions. *N Engl J Med* 1992;**327**:685–691.
5. The SOLVD Investigators. Effect of enalapril on survival in patients with reduced left ventricular ejection fractions and congestive heart failure. *N Engl J Med* 1991;**325**:293–302.
6. Yusuf S, Sleight P, Pogue J, Bosch J, Davies R, Dagenais G. Effects of an angiotensin-converting-enzyme inhibitor, ramipril, on cardiovascular events in high-risk patients. The Heart Outcomes Prevention Evaluation Study Investigators. *N Engl J Med* 2000;**342**:145–153.
7. Zannad F, McMurray JJ, Krum H, van Veldhuisen DJ, Swedberg K, Shi H, Vincent J, Pocock SJ, Pitt B. Eplerenone in patients with systolic heart failure and mild symptoms. *N Engl J Med* 2011;**364**:11–21.
8. Pitt B, Zannad F, Remme WJ, Cody R, Castaigne A, Perez A, Palensky J, Wittes J. The effect of spironolactone on morbidity and mortality in patients with severe heart failure. Randomized Aldactone Evaluation Study Investigators. *N Engl J Med* 1999;**341**:709–717.
9. Moss AJ, Hall WJ, Cannom DS, Daubert JP, Higgins SL, Klein H, Levine JH, Saksena S, Waldo AL, Wilber D, Brown MW, Heo M. Improved survival with an implanted defibrillator in patients with coronary disease at high risk for ventricular arrhythmia. Multicenter Automatic Defibrillator Implantation Trial Investigators. *N Engl J Med* 1996;**335**:1933–1940.
10. Bonow RO, Maurer G, Lee KL, Holly TA, Binkley PF, Desvigne-Nickens P, Drozdz J, Farsky PS, Feldman AM, Doenst T, Michler RE, Berman DS, Nicolau JC, Pellikka PA, Wrobel K, Alotti N, Asch FM, Favaloro LE, She L, Velazquez EJ, Jones RH, Panza JA. Myocardial viability and survival in ischemic left ventricular dysfunction. *N Engl J Med* 2011;**364**:1617–1625.
11. Cleland JG, Calvert M, Freemantle N, Arrow Y, Ball SG, Bonser RS, Chattopadhyay S, Norell MS, Pennell DJ, Senior R. The Heart Failure Revascularisation Trial (HEART). *Eur J Heart Fail* 2011;**13**:227–233.
12. D'Egidio G, Nichol G, Williams KA, Guo A, Garrard L, deKemp R, Ruddy TD, DaSilva J, Humen D, Gulenchyn KY, Freeman M, Racine N, Benard F, Hendry P, Beanlands RS. Increasing benefit from revascularization is associated with increasing amounts of myocardial hibernation: a substudy of the PARR-2 trial. *JACC Cardiovasc Imaging* 2009;**2**:1060–1068.

13. Stanton T, Leano R, Marwick TH. Prediction of all-cause mortality from global longitudinal speckle strain: comparison with ejection fraction and wall motion scoring. *Circ Cardiovasc Imaging* 2009;**2**:356–364.
14. Kalam K, Otahal P, Marwick TH. Prognostic implications of global LV dysfunction: a systematic review and meta-analysis of global longitudinal strain and ejection fraction. *Heart* 2014;**100**:1673–1680.
15. Gandy SJ, Waugh SA, Nicholas RS, Simpson HJ, Milne W, Houston JG. Comparison of the reproducibility of quantitative cardiac left ventricular assessments in healthy volunteers using different MRI scanners: a multicenter simulation. *J Magn Reson Imaging* 2008;**28**:359–365.
16. Myerson SG, Bellenger NG, Pennell DJ. Assessment of left ventricular mass by cardiovascular magnetic resonance. *Hypertension* 2002;**39**:750–755.
17. Geleijnse ML, Fioretti PM, Roelandt JR. Methodology, feasibility, safety and diagnostic accuracy of dobutamine stress echocardiography. *J Am Coll Cardiol* 1997;**30**: 595–606.
18. Senior R, Kenny A, Nihoyannopoulos P. Stress echocardiography for assessing myocardial ischaemia and viable myocardium. *Heart* 1997;**78(**Suppl. 1):12–18.
19. Chia KK, Picard MH, Skopicki HA, Hung J. Viability of hypokinetic segments: influence of tethering from adjacent segments: influence of tethering from adjacent segments. *Echocardiography* 2002;**19**:475–481.
20. Wei K, Jayaweera AR, Firoozan S, Linka A, Skyba DM, Kaul S. Quantification of myocardial blood flow with ultrasound-induced destruction of microbubbles administered as a constant venous infusion. *Circulation* 1998;**97**:473–483.
21. Al-Saadi N, Nagel E, Gross M, Bornstedt A, Schnackenburg B, Klein C, Klimek W, Oswald H, Fleck E. Noninvasive detection of myocardial ischemia from perfusion reserve based on cardiovascular magnetic resonance. *Circulation* 2000;**101**: 1379–1383.
22. Jerosch-Herold M. Quantification of myocardial perfusion by cardiovascular magnetic resonance. *J Cardiovasc Magn Reson* 2010;**12**:57.
23. Brown KA. Prognostic value of thallium-201 myocardial perfusion imaging. A diagnostic tool comes of age. *Circulation* 1991;**83**:363–381.
24. Ugander M, Oki AJ, Hsu LY, Kellman P, Greiser A, Aletras AH, Sibley CT, Chen MY, Bandettini WP, Arai AE. Extracellular volume imaging by magnetic resonance imaging provides insights into overt and sub-clinical myocardial pathology. *Eur Heart J* 2012;**33**:1268–1278.
25. Sado DM, Flett AS, Banypersad SM, White SK, Maestrini V, Quarta G, Lachmann RH, Murphy E, Mehta A, Hughes DA, McKenna WJ, Taylor AM, Hausenloy DJ, Hawkins PN, Elliott PM, Moon JC. Cardiovascular magnetic resonance measurement of myocardial extracellular volume in health and disease. *Heart* 2012;**98**:1436–1441.
26. Jennings RB, Reimer KA. The cell biology of acute myocardial ischemia. *Annu Rev Med* 1991;**42**:225–246.
27. Nagoshi T, Yoshimura M, Rosano GM, Lopaschuk GD, Mochizuki S. Optimization of cardiac metabolism in heart failure. *Curr Pharm Des* 2011;**17**:3846–3853.
28. Stanley WC, Recchia FA, Lopaschuk GD. Myocardial substrate metabolism in the normal and failing heart. *Physiol Rev* 2005;**85**:1093–1129.
29. Vliegen HW, van der Laarse A, Cornelisse CJ, Eulderink F. Myocardial changes in pressure overload-induced left ventricular hypertrophy. A study on tissue composition, polyploidization and multinucleation. *Eur Heart J* 1991;**12**:488–494.
30. Bishop JE, Lindahl G. Regulation of cardiovascular collagen synthesis by mechanical load. *Cardiovasc Res* 1999;**42**:27–44.
31. Dostal DE. Regulation of cardiac collagen: angiotensin and cross-talk with local growth factors. *Hypertension* 2001;**37**:841–844.
32. Lang RM, Bierig M, Devereux RB, Flachskampf FA, Foster E, Pellikka PA, Picard MH, Roman MJ, Seward J, Shanewise J, Solomon S, Spencer KT, St John Sutton M, Stewart W,Chamber Quantification Writing Group, American Society of Echocardiography's Guidelines and Standards Committee, European Association of Echocardiography. Recommendations for chamber quantification. *Eur J Echocardiogr* 2006;**7**:79–108.
33. Zagrosek A, Abdel-Aty H, Boye P, Wassmuth R, Messroghli D, Utz W, Rudolph A, Bohl S, Dietz R, Schulz-Menger J. Cardiac magnetic resonance monitors reversible and irreversible myocardial injury in myocarditis. *JACC Cardiovasc Imaging* 2009;**2**: 131–138.
34. von Knobelsdorff-Brenkenhoff F, Prothmann M, Dieringer MA, Wassmuth R, Greiser A, Schwenke C, Niendorf T, Schulz-Menger J. Myocardial T1 and T2 mapping at 3 T: reference values, influencing factors and implications. *J Cardiovasc Magn Reson* 2013;**15**:53.
35. Sdringola S, Johnson NP, Kirkeeide RL, Cid E, Gould KL. Impact of unexpected factors on quantitative myocardial perfusion and coronary flow reserve in young, asymptomatic volunteers. *JACC Cardiovasc Imaging* 2011;**4**:402–412.
36. Salerno M, Beller GA. Noninvasive assessment of myocardial perfusion. *Circ Cardiovasc Imaging* 2009;**2**:412–424.
37. Morton G, Chiribiri A, Ishida M, Hussain ST, Schuster A, Indermuehle A, Perera D, Knuuti J, Baker S, Hedstrom E, Schleyer P, O'Doherty M, Barrington S, Nagel E. Quantification of absolute myocardial perfusion in patients with coronary artery disease: comparison between cardiovascular magnetic resonance and positron emission tomography. *J Am Coll Cardiol* 2012;**60**:1546–1555.
38. Fritz-Hansen T, Hove JD, Kofoed KF, Kelbaek H, Larsson HB. Quantification of MRI measured myocardial perfusion reserve in healthy humans: a comparison with positron emission tomography. *J Magn Reson Imaging* 2008;**27**:818–824.
39. Reimer KA, Jennings RB. The "wavefront phenomenon" of myocardial ischemic cell death. II. Transmural progression of necrosis within the framework of ischemic bed size (myocardium at risk) and collateral flow. *Lab Invest* 1979;**40**: 633–644.
40. Braunwald E, Kloner RA. The stunned myocardium: prolonged, postischemic ventricular dysfunction. *Circulation* 1982;**66**:1146–1149.
41. Kloner RA, Braunwald E. Observations on experimental myocardial ischaemia. *Cardiovasc Res* 1980;**14**:371–395.
42. Lockie T, Nagel E, Redwood S, Plein S. Use of cardiovascular magnetic resonance imaging in acute coronary syndromes. *Circulation* 2009;**119**:1671–1681.
43. Krahwinkel W, Ketteler T, Godke J, Wolfertz J, Ulbricht LJ, Krakau I, Gulker H. Dobutamine stress echocardiography. *Eur Heart J* 1997;**18**(Suppl. D):D9–15.
44. Pack NA, DiBella EV, Rust TC, Kadrmas DJ, McGann CJ, Butterfield R, Christian PE, Hoffman JM. Estimating myocardial perfusion from dynamic contrast-enhanced CMR with a model-independent deconvolution method. *J Cardiovasc Magn Reson* 2008;**10**:52.
45. NICE. Myocardial perfusion scintigraphy for the diagnosis and management of angina and myocardial infarction. NICE technology Appraisal Guidance. https://www.nice.org.uk/guidance/ta73.
46. Shaw LJ, Berman DS, Maron DJ, Mancini GB, Hayes SW, Hartigan PM, Weintraub WS, O'Rourke RA, Dada M, Spertus JA, Chaitman BR, Friedman J, Slomka P, Heller GV, Germano G, Gosselin G, Berger P, Kostuk WJ, Schwartz RG, Knudtson M, Veledar E, Bates ER, McCallister B, Teo KK, Boden WE. Optimal medical therapy with or without percutaneous coronary intervention to reduce ischemic burden: results from the Clinical Outcomes Utilizing Revascularization and Aggressive Drug Evaluation (COURAGE) trial nuclear substudy. *Circulation* 2008;**117**:1283–1291.
47. Shaw LJ, Bairey Merz CN, Pepine CJ, Reis SE, Bittner V, Kelsey SF, Olson M, Johnson BD, Mankad S, Sharaf BL, Rogers WJ, Wessel TR, Arant CB, Pohost GM, Lerman A, Quyyumi AA, Sopko G. Insights from the NHLBI-Sponsored Women's Ischemia Syndrome Evaluation (WISE) Study: Part I: gender differences in traditional and novel risk factors, symptom evaluation, and gender-optimized diagnostic strategies. *J Am Coll Cardiol* 2006;**47**(3 Suppl.): S4–S20.
48. Abidov A, Bax JJ, Hayes SW, Hachamovitch R, Cohen I, Gerlach J, Kang X, Friedman JD, Germano G, Berman DS. Transient ischemic dilation ratio of the left ventricle is a significant predictor of future cardiac events in patients with otherwise normal myocardial perfusion SPECT. *J Am Coll Cardiol* 2003;**42**: 1818–1825.
49. Robinson VJ, Corley JH, Marks DS, Eberhardt LW, Eubig C, Burke GJ, Prisant LM. Causes of transient dilatation of the left ventricle during myocardial perfusion imaging. *Am J Roentgenol* 2000;**174**:1349–1352.
50. Bengel FM, Higuchi T, Javadi MS, Lautamaki R. Cardiac positron emission tomography. *J Am Coll Cardiol* 2009;**54**:1–15.
51. Gould KL, Johnson NP, Bateman TM, Beanlands RS, Bengel FM, Bober R, Camici PG, Cerqueira MD, Chow BJ, Di Carli MF, Dorbala S, Gewirtz H, Gropler RJ, Kaufmann PA, Knaapen P, Knuuti J, Merhige ME, Rentrop KP, Ruddy TD, Schelbert HR, Schindler TH, Schwaiger M, Sdringola S, Vitarello J, Williams KA Sr, Gordon D, Dilsizian V, Narula J. Anatomic versus physiologic assessment of coronary artery disease: guiding management decisions using positron-emission tomography (PET) as a physiologic tool. *J Am Coll Cardiol* 2013;**62**:1639–53.
52. Di Carli M, Czernin J, Hoh CK, Gerbaudo VH, Brunken RC, Huang SC, Phelps ME, Schelbert HR. Relation among stenosis severity, myocardial blood flow, and flow reserve in patients with coronary artery disease. *Circulation* 1995;**91**:1944–1951.
53. Duncker DJ, Schulz R, Ferrari R, Garcia-Dorado D, Guarnieri C, Heusch G, Verdouw PD. "Myocardial stunning" remaining questions. *Cardiovasc Res* 1998; **38**:549–558.
54. Miyamae M, Fujiwara H, Kida M, Yokota R, Tanaka M, Katsuragawa M, Hasegawa K, Ohura M, Koga K, Yabuuchi Y, Sasayama S. Preconditioning improves energy metabolism during reperfusion but does not attenuate myocardial stunning in porcine hearts. *Circulation* 1993;**88**:223–234.
55. Di Carli MF, Prcevski P, Singh TP, Janisse J, Ager J, Muzik O, Vander Heide R. Myocardial blood flow, function, and metabolism in repetitive stunning. *J Nucl Med* 2000;**41**:1227–1234.
56. Heyndrickx GR, Millard RW, McRitchie RJ, Maroko PR, Vatner SF. Regional myocardial functional and electrophysiological alterations after brief coronary artery occlusion in conscious dogs. *J Clin Invest* 1975;**56**:978–985.
57. Ito H, Tomooka T, Sakai N, Higashino Y, Fujii K, Katoh O, Masuyama T, Kitabatake A, Minamino T. Time course of functional improvement in stunned

myocardium in risk area in patients with reperfused anterior infarction. *Circulation* 1993;**87**:355–362.
58. Yagita A, Naka M, Yamamoto K, Doi Y, Imai K, Shiotani I, Akamatsu Y, Hishida E, Masuyama T, Kinoshita N. [Recovery process from myocardial stunning after transient ischemia: assessment with pulsed wave Doppler transmitral flow pattern]. *J Cardiol* 1997;**30**:293–298.
59. Azevedo CF, Amado LC, Kraitchman DL, Gerber BL, Osman NF, Rochitte CE, Edvardsen T, Lima JA. Persistent diastolic dysfunction despite complete systolic functional recovery after reperfused acute myocardial infarction demonstrated by tagged magnetic resonance imaging. *Eur Heart J* 2004;**25**:1419–1427.
60. Smart SC, Sawada S, Ryan T, Segar D, Atherton L, Berkovitz K, Bourdillon PD, Feigenbaum H. Low-dose dobutamine echocardiography detects reversible dysfunction after thrombolytic therapy of acute myocardial infarction. *Circulation* 1993;**88**:405–415.
61. Marinho NV, Keogh BE, Costa DC, Lammerstma AA, Ell PJ, Camici PG. Pathophysiology of chronic left ventricular dysfunction. New insights from the measurement of absolute myocardial blood flow and glucose utilization. *Circulation* 1996; **93**:737–744.
62. Ausma J, Cleutjens J, Thone F, Flameng W, Ramaekers F, Borgers M. Chronic hibernating myocardium: interstitial changes. *Mol Cell Biochem* 1995;**147**:35–42.
63. Rahimtoola SH, La Canna G, Ferrari R. Hibernating myocardium: another piece of the puzzle falls into place. *J Am Coll Cardiol* 2006;**47**:978–980.
64. Schwarz ER, Schoendube FA, Kostin S, Schmiedtke N, Schulz G, Buell U, Messmer BJ, Morrison J, Hanrath P, vom Dahl J. Prolonged myocardial hibernation exacerbates cardiomyocyte degeneration and impairs recovery of function after revascularization. *J Am Coll Cardiol* 1998;**31**:1018–1026.
65. Cwajg JM, Cwajg E, Nagueh SF, He ZX, Qureshi U, Olmos LI, Quinones MA, Verani MS, Winters WL, Zoghbi WA. End-diastolic wall thickness as a predictor of recovery of function in myocardial hibernation: relation to rest-redistribution T1-201 tomography and dobutamine stress echocardiography. *J Am Coll Cardiol* 2000;**35**:1152–1161.
66. Camici PG, Prasad SK, Rimoldi OE. Stunning, hibernation, and assessment of myocardial viability. *Circulation* 2008;**117**:103–114.
67. Wiggers H, Noreng M, Paulsen PK, Bottcher M, Egeblad H, Nielsen TT, Botker HE. Energy stores and metabolites in chronic reversibly and irreversibly dysfunctional myocardium in humans. *J Am Coll Cardiol* 2001;**37**:100–108.
68. Vanoverschelde JL, Wijns W, Depre C, Essamri B, Heyndrickx GR, Borgers M, Bol A, Melin JA. Mechanisms of chronic regional postischemic dysfunction in humans. New insights from the study of noninfarcted collateral-dependent myocardium. *Circulation* 1993;**87**:1513–1523.
69. Elsasser A, Schlepper M, Klovekorn WP, Cai WJ, Zimmermann R, Muller KD, Strasser R, Kostin S, Gagel C, Munkel B, Schaper W, Schaper J. Hibernating myocardium: an incomplete adaptation to ischemia. *Circulation* 1997;**96**:2920–2931.
70. Baer FM, Theissen P, Schneider CA, Voth E, Sechtem U, Schicha H, Erdmann E. Dobutamine magnetic resonance imaging predicts contractile recovery of chronically dysfunctional myocardium after successful revascularization. *J Am Coll Cardiol* 1998;**31**:1040–1048.
71. Shah DJ, Kim HW, James O, Parker M, Wu E, Bonow RO, Judd RM, Kim RJ. Prevalence of regional myocardial thinning and relationship with myocardial scarring in patients with coronary artery disease. *JAMA* 2013;**309**:909–918.
72. Cornel JH, Bax JJ, Elhendy A, Maat AP, Kimman GJ, Geleijnse ML, Rambaldi R, Boersma E, Fioretti PM. Biphasic response to dobutamine predicts improvement of global left ventricular function after surgical revascularization in patients with stable coronary artery disease: implications of time course of recovery on diagnostic accuracy. *J Am Coll Cardiol* 1998;**31**:1002–1010.
73. Larrazet F, Pellerin D, Prigent A, Daou D, Cohen L, Veyrat C. Quantitative analysis of hibernating myocardium by dobutamine tissue Doppler echocardiography. *Am J Cardiol* 2001;**88**:418–422.
74. Bountioukos M, Schinkel AF, Bax JJ, Rizzello V, Valkema R, Krenning BJ, Biagini E, Vourvouri EC, Roelandt JR, Poldermans D. Pulsed wave tissue Doppler imaging for the quantification of contractile reserve in stunned, hibernating, and scarred myocardium. *Heart* 2004;**90**:506–510.
75. Kim RJ, Wu E, Rafael A, Chen EL, Parker MA, Simonetti O, Klocke FJ, Bonow RO, Judd RM. The use of contrast-enhanced magnetic resonance imaging to identify reversible myocardial dysfunction. *N Engl J Med* 2000;**343**:1445–1453.
76. Cheng AS, Selvanayagam JB, Jerosch-Herold M, van Gaal WJ, Karamitsos TD, Neubauer S, Banning AP. Percutaneous treatment of chronic total coronary occlusions improves regional hyperemic myocardial blood flow and contractility: insights from quantitative cardiovascular magnetic resonance imaging. *JACC Cardiovasc Interv* 2008;**1**:44–53.
77. Beller GA, Ragosta M, Watson DD, Gimple LW. Myocardial thallium-201 scintigraphy for assessment of viability in patients with severe left ventricular dysfunction. *Am J Cardiol* 1992;**70**:18E–22E.
78. Mylonas I, Beanlands RS. Radionuclide imaging of viable myocardium: is it underutilized? *Curr Cardiovasc Imaging Rep* 2011;**4**:251–261.
79. Galassi AR, Tamburino C, Grassi R, Foti R, Mammana C, Virgilio A, Licciardello G, Musumeci S, Giuffrida G. Comparison of technetium 99m-tetrofosmin and thallium-201 single photon emission computed tomographic imaging for the assessment of viable myocardium in patients with left ventricular dysfunction. *J Nucl Cardiol* 1998;**5**:56–63.
80. Gunning MG, Anagnostopoulos C, Davies G, Knight CJ, Pennell DJ, Fox KM, Pepper J, Underwood SR. Simultaneous assessment of myocardial viability and function for the detection of hibernating myocardium using ECG-gated 99Tcm-tetrofosmin emission tomography: a comparison with 201Tl emission tomography combined with cine magnetic resonance imaging. *Nucl Med Commun* 1999;**20**:209–214.
81. Fath-Ordoubadi F, Beatt KJ, Spyrou N, Camici PG. Efficacy of coronary angioplasty for the treatment of hibernating myocardium. *Heart* 1999;**82**:210–216.
82. Anagnostopoulos C, Georgakopoulos A, Pianou N, Nekolla SG. Assessment of myocardial perfusion and viability by positron emission tomography. *Int J Cardiol* 2013;**167**:1737–1749.
83. Pagano D, Fath-Ordoubadi F, Beatt KJ, Townend JN, Bonser RS, Camici PG. Effects of coronary revascularisation on myocardial blood flow and coronary vasodilator reserve in hibernating myocardium. *Heart* 2001;**85**:208–212.
84. Becker M, Ocklenburg C, Altiok E, Futing A, Balzer J, Krombach G, Lysyansky M, Kuhl H, Krings R, Kelm M, Hoffmann R. Impact of infarct transmurality on layer-specific impairment of myocardial function: a myocardial deformation imaging study. *Eur Heart J* 2009;**30**:1467–1476.
85. Sjoli B, Orn S, Grenne B, Ihlen H, Edvardsen T, Brunvand H. Diagnostic capability and reproducibility of strain by Doppler and by speckle tracking in patients with acute myocardial infarction. *JACC Cardiovasc Imaging* 2009;**2**:24–33.
86. Pegg TJ, Selvanayagam JB, Jennifer J, Francis JM, Karamitsos TD, Dall'Armellina E, Smith KL, Taggart DP, Neubauer S. Prediction of global left ventricular functional recovery in patients with heart failure undergoing surgical revascularisation, based on late gadolinium enhancement cardiovascular magnetic resonance. *J Cardiovasc Magn Reson* 2010;**12**:56.
87. Kumar V, Abbas AK, Fausto N, Mitchell R. Robbins Basic Pathology. 9th ed. Philedelphia: Saunders, 2007.
88. Bonvini RF, Hendiri T, Camenzind E. Inflammatory response post-myocardial infarction and reperfusion: a new therapeutic target? *Eur Heart J Suppl* 2005;**7**(Suppl. I):127–136.
89. Jennings RB, Reimer KA. Lethal myocardial ischemic injury. *Am J Pathol* 1981;**102**: 241–255.
90. Fishbein MC, Maclean D, Maroko PR. The histopathologic evolution of myocardial infarction. *Chest* 1978;**73**:843–849.
91. Ertl G, Frantz S. Healing after myocardial infarction. *Cardiovasc Res* 2005;**66**: 22–32.
92. Hauser AM, Gangadharan V, Ramos RG, Gordon S, Timmis GC. Sequence of mechanical, electrocardiographic and clinical effects of repeated coronary artery occlusion in human beings: echocardiographic observations during coronary angioplasty. *J Am Coll Cardiol* 1985;**5**(2 Pt 1):193–197.
93. Derumeaux G, Ovize M, Loufoua J, Andre-Fouet X, Minaire Y, Cribier A, Letac B. Doppler tissue imaging quantitates regional wall motion during myocardial ischemia and reperfusion. *Circulation* 1998;**97**:1970–1977.
94. Cheitlin MD, Armstrong WF, Aurigemma GP, Beller GA, Bierman FZ, Davis JL, Douglas PS, Faxon DP, Gillam LD, Kimball TR, Kussmaul WG, Pearlman AS, Philbrick JT, Rakowski H, Thys DM, Antman EM, Smith SC Jr, Alpert JS, Gregoratos G, Anderson JL, Hiratzka LF, Hunt SA, Fuster V, Jacobs AK, Gibbons RJ, Russell RO. ACC/AHA/ASE 2003 guideline update for the clinical application of echocardiography: summary article: a report of the American College of Cardiology/American Heart Association Task Force on Practice Guidelines (ACC/AHA/ASE Committee to Update the 1997 Guidelines for the Clinical Application of Echocardiography). *Circulation* 2003;**108**:1146–1162.
95. Chan J, Hanekom L, Wong C, Leano R, Cho GY, Marwick TH. Differentiation of subendocardial and transmural infarction using two-dimensional strain rate imaging to assess short-axis and long-axis myocardial function. *J Am Coll Cardiol* 2006;**48**:2026–2033.
96. Friedrich MG. Tissue characterization of acute myocardial infarction and myocarditis by cardiac magnetic resonance. *JACC Cardiovasc Imaging* 2008;**1**:652–662.
97. Friedrich MG, Abdel-Aty H, Taylor A, Schulz-Menger J, Messroghli D, Dietz R. The salvaged area at risk in reperfused acute myocardial infarction as visualized by cardiovascular magnetic resonance. *J Am Coll Cardiol* 2008;**51**:1581–1587.
98. Abdel-Aty H, Cocker M, Meek C, Tyberg JV, Friedrich MG. Edema as a very early marker for acute myocardial ischemia: a cardiovascular magnetic resonance study. *J Am Coll Cardiol* 2009;**53**:1194–1201.
99. Mather AN, Fairbairn TA, Artis NJ, Greenwood JP, Plein S. Timing of cardiovascular MR imaging after acute myocardial infarction: effect on estimates of infarct characteristics and prediction of late ventricular remodeling. *Radiology* 2011; **261**:116–126.

100. Orn S, Manhenke C, Greve OJ, Larsen AI, Bonarjee VV, Edvardsen T, Dickstein K. Microvascular obstruction is a major determinant of infarct healing and subsequent left ventricular remodelling following primary percutaneous coronary intervention. *Eur Heart J* 2009;**30**:1978–1985.
101. Kumar A, Green JD, Sykes JM, Ephrat P, Carson JJ, Mitchell AJ, Wisenberg G, Friedrich MG. Detection and quantification of myocardial reperfusion hemorrhage using T2*-weighted CMR. *JACC Cardiovasc Imaging* 2011;**4**:1274–1283.
102. Ganame J, Messalli G, Dymarkowski S, Rademakers FE, Desmet W, Van de Werf F, Bogaert J. Impact of myocardial haemorrhage on left ventricular function and remodelling in patients with reperfused acute myocardial infarction. *Eur Heart J* 2009;**30**:1440–1449.
103. Wolfe CL, Lewis SE, Corbett JR, Parkey RW, Buja LM, Willerson JT. Measurement of myocardial infarction fraction using single photon emission computed tomography. *J Am Coll Cardiol* 1985;**6**:145–151.
104. Wagner A, Mahrholdt H, Holly TA, Elliott MD, Regenfus M, Parker M, Klocke FJ, Bonow RO, Kim RJ, Judd RM. Contrast-enhanced MRI and routine single photon emission computed tomography (SPECT) perfusion imaging for detection of subendocardial myocardial infarcts: an imaging study. *Lancet* 2003;**361**:374–379.
105. Schwaiger M, Brunken R, Grover-McKay M, Krivokapich J, Child J, Tillisch JH, Phelps ME, Schelbert HR. Regional myocardial metabolism in patients with acute myocardial infarction assessed by positron emission tomography. *J Am Coll Cardiol* 1986;**8**:800–808.
106. Neumann FJ, Kosa I, Dickfeld T, Blasini R, Gawaz M, Hausleiter J, Schwaiger M, Schomig A. Recovery of myocardial perfusion in acute myocardial infarction after successful balloon angioplasty and stent placement in the infarct-related coronary artery. *J Am Coll Cardiol* 1997;**30**:1270–1276.
107. Klein C, Nekolla SG, Bengel FM, Momose M, Sammer A, Haas F, Schnackenburg B, Delius W, Mudra H, Wolfram D, Schwaiger M. Assessment of myocardial viability with contrast-enhanced magnetic resonance imaging: comparison with positron emission tomography. *Circulation* 2002;**105**:162–167.
108. Davila-Roman VG, Vedala G, Herrero P, de las Fuentes L, Rogers JG, Kelly DP, Gropler RJ. Altered myocardial fatty acid and glucose metabolism in idiopathic dilated cardiomyopathy. *J Am Coll Cardiol* 2002;**40**:271–277.
109. Chandler MP, Kerner J, Huang H, Vazquez E, Reszko A, Martini WZ, Hoppel CL, Imai M, Rastogi S, Sabbah HN, Stanley WC. Moderate severity heart failure does not involve a downregulation of myocardial fatty acid oxidation. *Am J Physiol Heart Circ Physiol* 2004;**287**:H1538–H1543.
110. Taylor M, Wallhaus TR, Degrado TR, Russell DC, Stanko P, Nickles RJ, Stone CK. An evaluation of myocardial fatty acid and glucose uptake using PET with [18F]fluoro-6-thia-heptadecanoic acid and [18F]FDG in patients with congestive heart failure. *J Nucl Med* 2001;**42**:55–62.
111. Varnava AM, Elliott PM, Baboonian C, Davison F, Davies MJ, McKenna WJ. Hypertrophic cardiomyopathy: histopathological features of sudden death in cardiac troponin T disease. *Circulation* 2001;**104**:1380–1384.
112. Unverferth DV, Fetters JK, Unverferth BJ, Leier CV, Magorien RD, Arn AR, Baker PB. Human myocardial histologic characteristics in congestive heart failure. *Circulation* 1983;**68**:1194–1200.
113. Brilla CG, Rupp H, Funck R, Maisch B. The renin-angiotensin-aldosterone system and myocardial collagen matrix remodelling in congestive heart failure. *Eur Heart J* 1995;**16**(Suppl. O):107–109.
114. Heeneman S, Cleutjens JP, Faber BC, Creemers EE, van Suylen RJ, Lutgens E, Cleutjens KB, Daemen MJ. The dynamic extracellular matrix: intervention strategies during heart failure and atherosclerosis. *J Pathol* 2003;**200**:516–525.
115. Weber KT, Sun Y, Tyagi SC, Cleutjens JP. Collagen network of the myocardium: function, structural remodeling and regulatory mechanisms. *J Mol Cell Cardiol* 1994;**26**:279–292.
116. Martos R, Baugh J, Ledwidge M, O'Loughlin C, Conlon C, Patle A, Donnelly SC, McDonald K. Diastolic heart failure: evidence of increased myocardial collagen turnover linked to diastolic dysfunction. *Circulation* 2007;**115**:888–895.
117. Curtis JP, Sokol SI, Wang Y, Rathore SS, Ko DT, Jadbabaie F, Portnay EL, Marshalko SJ, Radford MJ, Krumholz HM. The association of left ventricular ejection fraction, mortality, and cause of death in stable outpatients with heart failure. *J Am Coll Cardiol* 2003;**42**:736–742.
118. Lee TH, Hamilton MA, Stevenson LW, Moriguchi JD, Fonarow GC, Child JS, Laks H, Walden JA. Impact of left ventricular cavity size on survival in advanced heart failure. *Am J Cardiol* 1993;**72**:672–676.
119. Duncan AM, Francis DP, Gibson DG, Henein MY. Differentiation of ischemic from nonischemic cardiomyopathy during dobutamine stress by left ventricular long-axis function: additional effect of left bundle-branch block. *Circulation* 2003;**108**:1214–1220.
120. Afonso L, Kondur A, Simegn M, Niraj A, Hari P, Kaur R, Ramappa P, Pradhan J, Bhandare D, Williams KA, Zalawadiya S, Pinheiro A, Abraham TP. Two-dimensional strain profiles in patients with physiological and pathological hypertrophy and preserved left ventricular systolic function: a comparative analyses. *BMJ Open* 2012;**2**:e001390.
121. Maron BJ. Distinguishing hypertrophic cardiomyopathy from athlete's heart: a clinical problem of increasing magnitude and significance. *Heart* 2005;**91**:1380–1382.
122. Ommen SR, Nishimura RA, Appleton CP, Miller FA, Oh JK, Redfield MM, Tajik AJ. Clinical utility of Doppler echocardiography and tissue Doppler imaging in the estimation of left ventricular filling pressures: A comparative simultaneous Doppler-catheterization study. *Circulation* 2000;**102**:1788–1794.
123. Cao JJ, Wang Y, McLaughlin J, Haag E, Rhee P, Passick M, Toole R, Cheng J, Berke AD, Lachman J, Reichek N. Left ventricular filling pressure assessment using left atrial transit time by cardiac magnetic resonance imaging. *Circ Cardiovasc Imaging* 2011;**4**:130–138.
124. Leyva F, Taylor RJ, Foley PW, Umar F, Mulligan LJ, Patel K, Stegemann B, Haddad T, Smith RE, Prasad SK. Left ventricular midwall fibrosis as a predictor of mortality and morbidity after cardiac resynchronization therapy in patients with nonischemic cardiomyopathy. *J Am Coll Cardiol* 2012;**60**:1659–1667.
125. Adabag AS, Maron BJ, Appelbaum E, Harrigan CJ, Buros JL, Gibson CM, Lesser JR, Hanna CA, Udelson JE, Manning WJ, Maron MS. Occurrence and frequency of arrhythmias in hypertrophic cardiomyopathy in relation to delayed enhancement on cardiovascular magnetic resonance. *J Am Coll Cardiol* 2008;**51**:1369–1374.
126. Roes SD, Kelle S, Kaandorp TA, Kokocinski T, Poldermans D, Lamb HJ, Boersma E, van der Wall EE, Fleck E, de Roos A, Nagel E, Bax JJ. Comparison of myocardial infarct size assessed with contrast-enhanced magnetic resonance imaging and left ventricular function and volumes to predict mortality in patients with healed myocardial infarction. *Am J Cardiol* 2007;**100**:930–936.
127. Iles L, Pfluger H, Phrommintikul A, Cherayath J, Aksit P, Gupta SN, Kaye DM, Taylor AJ. Evaluation of diffuse myocardial fibrosis in heart failure with cardiac magnetic resonance contrast-enhanced T1 mapping. *J Am Coll Cardiol* 2008;**52**:1574–1580.
128. Banypersad SM, Sado DM, Flett AS, Gibbs SD, Pinney JH, Maestrini V, Cox AT, Fontana M, Whelan CJ, Wechalekar AD, Hawkins PN, Moon JC. Quantification of myocardial extracellular volume fraction in systemic AL amyloidosis: an equilibrium contrast cardiovascular magnetic resonance study. *Circ Cardiovasc Imaging* 2013;**6**:34–39.
129. Anderson LJ, Holden S, Davis B, Prescott E, Charrier CC, Bunce NH, Firmin DN, Wonke B, Porter J, Walker JM, Pennell DJ. Cardiovascular T2-star (T2*) magnetic resonance for the early diagnosis of myocardial iron overload. *Eur Heart J* 2001;**22**:2171–2179.
130. Yao SS, Qureshi E, Nichols K, Diamond GA, Depuey EG, Rozanski A. Prospective validation of a quantitative method for differentiating ischemic versus nonischemic cardiomyopathy by technetium-99m sestamibi myocardial perfusion single-photon emission computed tomography. *Clin Cardiol* 2004;**27**:615–620.
131. Wu YW, Yen RF, Chieng PU, Huang PJ. Tl-201 myocardial SPECT in differentiation of ischemic from nonischemic dilated cardiomyopathy in patients with left ventricular dysfunction. *J Nucl Cardiol* 2003;**10**:369–374.
132. Knaapen P, Gotte MJ, Paulus WJ, Zwanenburg JJ, Dijkmans PA, Boellaard R, Marcus JT, Twisk JW, Visser CA, van Rossum AC, Lammertsma AA, Visser FC. Does myocardial fibrosis hinder contractile function and perfusion in idiopathic dilated cardiomyopathy? PET and MR imaging study. *Radiology* 2006;**240**:380–388.
133. van den Heuvel AF, van Veldhuisen DJ, van der Wall EE, Blanksma PK, Siebelink HM, Vaalburg WM, van Gilst WH, Crijns HJ. Regional myocardial blood flow reserve impairment and metabolic changes suggesting myocardial ischemia in patients with idiopathic dilated cardiomyopathy. *J Am Coll Cardiol* 2000;**35**:19–28.
134. de Jong RM, Tio RA, van der Harst P, Voors AA, Koning PM, Zeebregts CJ, van Veldhuisen DJ, Dierckx RA, Slart RH. Ischemic patterns assessed by positron emission tomography predict adverse outcome in patients with idiopathic dilated cardiomyopathy. *J Nucl Cardiol* 2009;**16**:769–774.
135. Montalescot G, Sechtem U, Achenbach S, Andreotti F, Arden C, Budaj A, Bugiardini R, Crea F, Cuisset T, Di Mario C, Ferreira JR, Gersh BJ, Gitt AK, Hulot JS, Marx N, Opie LH, Pfisterer M, Prescott E, Ruschitzka F, Sabate M, Senior R, Taggart DP, van der Wall EE, Vrints CJ, Zamorano JL, Baumgartner H, Bax JJ, Bueno H, Dean V, Deaton C, Erol C, Fagard R, Ferrari R, Hasdai D, Hoes AW, Kirchhof P, Knuuti J, Kolh P, Lancellotti P, Linhart A, Nihoyannopoulos P, Piepoli MF, Ponikowski P, Sirnes PA, Tamargo JL, Tendera M, Torbicki A, Wijns W, Windecker S, Valgimigli M, Claeys MJ, Donner-Banzhoff N, Frank H, Funck-Brentano C, Gaemperli O, Gonzalez-Juanatey JR, Hamilos M, Husted S, James SK, Kervinen K, Kristensen SD, Maggioni AP, Pries AR, Romeo F, Ryden L, Simoons ML, Steg PG, Timmis A, Yildirir A. 2013 ESC guidelines on the management of stable coronary artery disease: The Task Force on the management of stable coronary artery disease of the European Society of Cardiology. *Eur Heart J* 2013;**34**:2949–3003.
136. Senior R, Becher H, Monaghan M, Agati L, Zamorano J, Vanoverschelde JL, Nihoyannopoulos P. Contrast echocardiography: evidence-based

recommendations by European Association of Echocardiography. *Eur J Echocardiogr* 2009;**10**:194–212.
137. Picano E, Lattanzi F, Orlandini A, Marini C, L'Abbate A. Stress echocardiography and the human factor: the importance of being expert. *J Am Coll Cardiol* 1991;**17**: 666–669.
138. Baggish AL, Boucher CA. Radiopharmaceutical agents for myocardial perfusion imaging. *Circulation* 2008;**118**:1668–1674.
139. Crean A, Khan SN, Davies LC, Coulden R, Dutka DP. Assessment of myocardial scar: comparison between F-FDG PET, CMR and Tc-Sestamibi. *Clin Med Cardiol* 2009;**3**:69–76.
140. Berman DS, Kang X, Slomka PJ, Gerlach J, de Yang L, Hayes SW, Friedman JD, Thomson LE, Germano G. Underestimation of extent of ischemia by gated SPECT myocardial perfusion imaging in patients with left main coronary artery disease. *J Nucl Cardiol* 2007;**14**:521–528.
141. Plana JC, Mikati IA, Dokainish H, Lakkis N, Abukhalil J, Davis R, Hetzell BC, Zoghbi WA. A randomized cross-over study for evaluation of the effect of image optimization with contrast on the diagnostic accuracy of dobutamine echocardiography in coronary artery disease The OPTIMIZE Trial. *JACC Cardiovasc Imaging* 2008;**1**:145–152.
142. Seo Y, Mari C, Hasegawa BH. Technological development and advances in single-photon emission computed tomography/computed tomography. *Semin Nucl Med* 2008;**38**:177–198.
143. Greenwood JP, Maredia N, Younger JF, Brown JM, Nixon J, Everett CC, Bijsterveld P, Ridgway JP, Radjenovic A, Dickinson CJ, Ball SG, Plein S. Cardiovascular magnetic resonance and single-photon emission computed tomography for diagnosis of coronary heart disease (CE-MARC): a prospective trial. *Lancet* 2012; **379**:453–460.
144. Shan K, Bick RJ, Poindexter BJ, Shimoni S, Letsou GV, Reardon MJ, Howell JF, Zoghbi WA, Nagueh SF. Relation of tissue Doppler derived myocardial velocities to myocardial structure and beta-adrenergic receptor density in humans. *J Am Coll Cardiol* 2000;**36**:891–896.
145. Chang J, Nair V, Luk A, Butany J. Pathology of myocardial infarction. *Diagn Histopathol* 2013;**19**:1–28.
146. Hughes SE. The pathology of hypertrophic cardiomyopathy. *Histopathology* 2004; **44**:412–427.
147. Asimaki A, Saffitz JE. The role of endomyocardial biopsy in ARVC: looking beyond histology in search of new diagnostic markers. *J Cardiovasc Electrophysiol* 2011;**22**: 111–117.
148. Gulati A, Jabbour A, Ismail TF, Guha K, Khwaja J, Raza S, Morarji K, Brown TD, Ismail NA, Dweck MR, Di Pietro E, Roughton M, Wage R, Daryani Y, O'Hanlon R, Sheppard MN, Alpendurada F, Lyon AR, Cook SA, Cowie MR, Assomull RG, Pennell DJ, Prasad SK. Association of fibrosis with mortality and sudden cardiac death in patients with nonischemic dilated cardiomyopathy. *JAMA* 2013;**309**:896–908.
149. McDiarmid AK, Loh H, Nikitin N, Cleland JG, Ball SG, Greenwood JP, Plein S, Sparrow P. Predictive power of late gadolinium enhancement for myocardial recovery in chronic ischaemic heart failure: a HEART sub-study. *ESC Heart Failure* 2014;**1**: 146–153.
150. Velazquez EJ, Lee KL, Deja MA, Jain A, Sopko G, Marchenko A, Ali IS, Pohost G, Gradinac S, Abraham WT, Yii M, Prabhakaran D, Szwed H, Ferrazzi P, Petrie MC, O'Connor CM, Panchavinnin P, She L, Bonow RO, Rankin GR, Jones RH, Rouleau JL; STICH Investigators. Coronary-artery bypass surgery in patients with left ventricular dysfunction. *N Engl J Med* 2011;**364**:1607–1616.